bioRxiv preprint doi: https://doi.org/10.1101/2025.02.07.637049; this version posted February 7, 2025. The copyright holder for this preprint (which was not certified by peer review) is the author/funder, who has granted bioRxiv a license to display the preprint in perpetuity. It is made available under aCC-BY-NC 4.0 International license.

Experimentally mimicking 30 years of *Magallana gigas* infections with the OsHV-1 virus reveals evolution through positive selection

Camille Pelletier[1], Nicole Faury[1], Mickaël Mege[1,#], Lionel Dégremont[1], Maelle Hattinguais[1], Jeremie Vidal-Dupiol[2], Germain Chevignon[1], Maude Jacquot[1,*], Benjamin Morga[1,*]

Affiliations

[1] Ifremer, RBE-ASIM, Unité Adaptations Santé des Invertébrés Marins, Avenue de Mus de Loup, 17390 La Tremblade, France.

[2] IHPE, Univ Montpellier, CNRS, IFREMER, Univ Perpignan Via Domitia, Montpellier, France

Current address: INRAE, UMR BIOEPAR, TiBoDi Team, Oniris – site de la Chantrerie, Route de Gachet - CS40706, 44307 Nantes cedex 3

*Corresponding authors:

- Benjamin Morga; E-mail address: benjamin.morga@ifremer.fr; Tel: +33 5 46 76 26 49

- Maude Jacquot; E-mail address: maude.jacquot@ifremer.fr; Tel: +33 5 46 76 26 82

bioRxiv preprint doi: https://doi.org/10.1101/2025.02.07.637049; this version posted February 7, 2025. The copyright holder for this preprint (which was not certified by peer review) is the author/funder, who has granted bioRxiv a license to display the preprint in perpetuity. It is made available under aCC-BY-NC 4.0 International license.

Abstract

Ostreid herpesvirus 1 (OsHV-1) poses a significant threat to the global oyster farming industry, causing substantial economic losses due to mortality outbreaks. While OsHV-1 primarily affects the Pacific oyster *Magallana gigas*, it has been linked to mortality events in various host species. Despite advancements in understanding OsHV-1 epidemiology, knowledge gaps persist regarding its evolutionary mechanisms and adaptation to host genetic backgrounds. This study employs experimental evolution and extensive genomic analysis to unravel the dynamics of OsHV-1 evolution in response to oyster host genetic variation. Our results show that genetic mutations, particularly transitions and transversions, played a significant role in shaping the viral population, leading to a trend toward genetic homogenization. Stronger positive selection signals were observed in the oyster population with higher susceptibility, suggesting adaptation of viral genotypes to specific host genetic backgrounds. These findings shed light on the complex evolutionary dynamics of OsHV-1 and its interactions with oyster hosts. Understanding how this virus adapts to host genetic diversity is crucial for developing strategies to mitigate its impact on the oyster farming industry and provides valuable insights into the broader mechanisms of viral evolution in response to host variation.

bioRxiv preprint doi: https://doi.org/10.1101/2025.02.07.637049; this version posted February 7, 2025. The copyright holder for this preprint (which was not certified by peer review) is the author/funder, who has granted bioRxiv a license to display the preprint in perpetuity. It is made available under aCC-BY-NC 4.0 International license.

Introduction

Ostreid herpesvirus 1 (OsHV-1), a double-stranded DNA virus belonging to the *Malacoherpesviridae*, poses a significant threat to the global oyster farming industry by initiating a polymicrobial diseases, the Pacific Oyster Mortality Syndrome (POMS, de Lorgeril et al., 2018). In recent years, mortality outbreaks associated with the POMS have caused substantial economic losses. Among several factors (i.e. temperature and food) driving windows of oyster permissivity to diseases oyster age is essential with individuals being susceptible up to ~18 month old (Azéma, Lamy, et al., 2017; Burioli et al., 2017; Nicolas et al., 1992; Renault et al., 1994). Meanwhile, oyster farmers reported mortality associated with OsHV-1 mainly in spat, as survivors demonstrate genetic and epigenetic resistance upon subsequent exposure to the virus (Evans et al., 2017; Gawra et al., 2023).

The first comprehensive characterization of the OsHV-1 genome was published in 2005 (Davison et al., 2005). The genome of OsHV-1 spans approximately 207 kilobase pairs (kb) in length and exhibits a distinctive genomic organization comprising unique regions (U_L/U_S: unique long or short) flanked by repeated regions (TR_L/TR_S: terminal repeat long or short and IR_L/IR_S: inverted repeat long or short). The architecture of the OsHV-1 genome can be summarized as TR_L-U_L-IR_L-X-IR_S-U_S-TR_S (Davison et al., 2005). Advances in high-throughput sequencing have facilitated the genomic characterization of several OsHV-1 genotypes, including OsHV-1 µVar (Burioli et al., 2017), OsHV-1 PT (Abbadi et al., 2018), and OsHV-1 SB (Xia et al., 2015). Currently, 28 complete genomes are available in public databases (Delmotte-Pelletier et al., 2022; Morga-Jacquot et al., 2021, Pelletier et al., 2024)). These genomic datasets have revealed a spatiotemporal structuration of viral genotypes in France (Delmotte-Pelletier et al., 2022) and globally (Morga-Jacquot et al., 2021), consistent with oyster farming practices. Furthermore, a recent study has highlighted differentiation between genotypes infecting *M. gigas* and *O. edulis*, with a greater viral diversity observed in *M. gigas* (Pelletier et al., 2024). However, despite significant advancements in understanding OsHV-1 epidemiological and evolutionary processes, several knowledge gaps persist regarding its evolutionary mechanisms and how it adapts to host genetic backgrounds. Indeed, substantial genetic and epigenetic variation for resistance to OsHV-1 has been reported worldwide allowing selective breeding program to sustain oyster production (Camara et al.,

bioRxiv preprint doi: https://doi.org/10.1101/2025.02.07.637049; this version posted February 7, 2025. The copyright holder for this preprint (which was not certified by peer review) is the author/funder, who has granted bioRxiv a license to display the preprint in perpetuity. It is made available under aCC-BY-NC 4.0 International license.

2017; Dégremont et al., 2015b; Divilov et al., 2019; Gutierrez et al., 2020, Gawra et al., 2023; Valdivieso et al., 2025).

The evolution of viruses is driven by a range of processes, including mutation, genetic recombination, genetic drift and natural selection. RNA viruses provide vivid examples of high mutation rates and rapid evolution. These viruses are known for their ability to accumulate genetic changes swiftly, resulting in substantial levels of viral polymorphism (Sanjuán, 2012; Sanjuán & Domingo-Calap, 2016, 2016). This genetic diversity empowers them to adapt to newly infected cellular environments and develop strategies to evade vaccines and antiviral drugs (Lauring, 2020). Although large dsDNA viruses exhibit lower mutation rates (*i.e.* between 10^{-03} and 10^{-08} nucleotide substitution/site/year, e.g. $5.9x10^{-08}$ for the Herpes simplex virus) compared to RNA viruses (i.e. between 10^{-02} and 10^{-04} nucleotide substitution/site/year) due to their use of high-fidelity proofreading polymerases (Sanjuán, 2012; Sanjuán et al., 2010; Sanjuán & Domingo-Calap, 2016), their genome stability is increasingly controversial because they sometimes display noteworthy genetic diversity (Sanjuán et al., 2016).

Viral evolutionary processes can be investigated through various approaches including sequence analyses, metagenomics, phylogenetics, phylodynamics, and even Experimental Evolution (EE). This former approach involves subjecting viruses to controlled laboratory conditions, enabling the real-time observation and manipulation of evolutionary processes (Kawecki et al., 2012). The emergence and dynamics of mutations, immune escape variants, and evolutionary trade-offs could be assessed by monitoring viral populations under different selective pressures, such as antiviral drug treatments or interactions with immune systems (Kawecki et al., 2012).

While most studies using EE focus on easily replicable model organisms such as *Escherichia coli*, *Drosophila spp*, *Saccharomyces cerevisiae* or various bacteriophages (Kawecki et al., 2012), recent research has expanded EE to diverse viruses, including Herpesviruses (Fuandila et al., 2022; Kuny et al., 2020).

For instance, *in vitro* EE conducted with populations of Herpes Simplex Virus type 1 (HSV-1) have revealed the accumulation of minor genetic variants and changes in population diversity. Although

bioRxiv preprint doi: https://doi.org/10.1101/2025.02.07.637049; this version posted February 7, 2025. The copyright holder for this preprint (which was not certified by peer review) is the author/funder, who has granted bioRxiv a license to display the preprint in perpetuity. It is made available under aCC-BY-NC 4.0 International license.

minor, these changes have been observed to lead to relatively rapid modifications in the viral population at the consensus level (Kuny et al., 2020). Another EE study, conducted on Koi herpesvirus (KHV), which infects the common carp *Cyprinus carpio*, has highlighted the key role of structural variations in the rapid virus evolution *in vitro* (Fuandila et al., 2022). By driving genetic diversity, adaptation, and pathogenicity changes, these large-scale genomic alterations, including deletions, insertions, duplications, and inversions, can rapidly reshape viral genomes, influencing key functional regions (Fuandila et al., 2022).

In the absence of oyster cell lines for OsHV-1 propagation, we were forced to use *in vivo* techniques requiring high-throughput sequencing to efficiently and comprehensively analyze the evolution of viral populations. This however offer the advantage to study this host pathogen interaction as a whole in an ecologically relevant experiment.

In the context of OsHV-1, our understanding of the evolutionary processes contributing to the diversity of the viral population remains limited. The primary objective of the present study is to gain insights into the evolutionary mechanisms driving the adaptation and diversification of the OsHV-1 genotypes based on infection susceptibility of oysters. To achieve this goal, we used an EE approach spanning up to 28 generations under controlled conditions, combined with a comprehensive sequencing analysis of 90 OsHV-1 genomes.

Material and methods

Oysters production

To explore the impact of oyster genetic backgrounds on the evolutionary dynamics of OsHV-1, three oyster populations with varying levels of resistance against OsHV-1 infection were generated. In December 2021, wild oysters were collected from two sites in Charente-Maritime (France) based on their proximity to oyster farms.

bioRxiv preprint doi: https://doi.org/10.1101/2025.02.07.637049; this version posted February 7, 2025. The copyright holder for this preprint (which was not certified by peer review) is the author/funder, who has granted bioRxiv a license to display the preprint in perpetuity. It is made available under aCC-BY-NC 4.0 International license.

The first site, La Floride (Marennes-Oléron bay, Charente-Maritime, Lat: 45.803; Long.: -1.153) is located in an area surrounded by oyster farms and densely populated by wild oyster beds. It is annually exposed to OsHV-1 infections (Dégremont et al., 2019). This population is highly resistant to POMS (Valdivieso et al., 2025).

The second site, Chaucre (Charente-maritime, Lat: 45.982; Long: -1.396), is located on the West coast of Oléron island in a non-farming area where wild oyster beds are lowly populated. Oysters collected from Chaucre are less likely to be annualy infected with OsHV-1 than oysters from densely populated area and may therefore be moderately susceptible to OsHV-1 infection.

Moreover, a control oyster population currently used in other studies was included in our experiment (Gawra et al., 2023; Valdivieso et al., 2025). These oysters were initially sampled in 2008 before the emergence of OsHV-1 µVar, and since 2009, they have been reproduced over six successive generations using oysters from the second generation that have never been exposed to OsHV-1. Therefore, it can be assumed that this oyster population is naive to OsHV-1 since 2009, as animals have always been kept in a secured facility using UV-treated seawater (40 mj/cm^2). This population has been described as highly susceptible to OsHV-1, with mortality exceeding 80% (Valdivieso et al., 2025).

The three oyster populations (La Floride, Chaucre, and a naïve population) were housed separately at the Ifremer hatchery in La Tremblade (December 2021) to prevent potential pathogen transmission (OsHV-1, *Vibrio aestuarianus*) (Dégremont et al., 2005). Seawater temperature was raised from 11°C to 20°C and maintained under a cultured phytoplankton diet (*Isochrysis galbana*, *Tetraselmis suecica* and *Skeletonema costatum*) to induce gametogenesis (Dégremont et al., 2005).

In March 2022, 30 oysters per population were sexed, and gametes were collected via gonad stripping. Female gametes were pooled, filtered (20-µm and 100-µm screens), and fertilized with sperm collected individually from males. After 10 minutes, all eggs were combined and transferred to 30 L tanks to minimize sperm competition and maximize effective population size (Boudry et al., 2002). Larval and spat culture followed established protocols (Dégremont et al., 2005, 2007). Progenies were maintained in UV-treated seawater before experimental OsHV-1 infections and renamed FA, NFA, and C, denoting

bioRxiv preprint doi: https://doi.org/10.1101/2025.02.07.637049; this version posted February 7, 2025. The copyright holder for this preprint (which was not certified by peer review) is the author/funder, who has granted bioRxiv a license to display the preprint in perpetuity. It is made available under aCC-BY-NC 4.0 International license.

141 farming area (high density with the typical oyster bed of hundreds individuals/m² and annual POMS
142 reported), non-farming area (low density, less than 20 individuals/m² and no POMS reported), and
143 control populations (laboratory population, highly sensitive to OsHV-1 infection).

144 Before the experiment, spat were acclimated in 120 L tanks with a continuous flow of UV-filtered
145 seawater heated at 19°C. The seawater was enriched with a phytoplankton mixture containing *I.*
146 *galbana, T. suecica* and *S. costatum*. The acclimation process spanned at least 2 weeks to ensure optimal
147 growth and feeding conditions, essential for effective virus replication and oyster mortalities (Azéma,
148 Maurouard, et al., 2017).

149 ## Viral suspension preparation

150 To generate a diversified viral inoculum for infecting all oyster populations, nine viral suspensions were
151 produced between the years 2020 and 2021. These viral suspensions were generated using spat oysters
152 collected during monitoring of OsHV-1 infections from various areas in France. Briefly, approximately
153 1000 specific-pathogen-free (SPF) spat oysters, reared in the Ifremer experimental facilities located in
154 Argenton (Brittany, France), following a standardized methodology (Petton et al., 2015), were deployed
155 into four oyster farming areas during periods of disease outbreaks (Figure 1). These areas included *i)*
156 Brest harbor (BR) (used to produce 2 viral suspensions) (Logonna-Daoulas, lat.: 48.335 long.: -4.318),
157 *ii)* Marennes-Oléron bay (MO) (used to produce 4 viral suspensions) (La Floride, lat.: 45.803 and long.:
158 -1.153), *iii)* Arcachon basin (ARC) (used to produce 2 viral suspensions) (Grahude, lat.: 44.653 and
159 long.: -1.073), *iv)* Leucate lagoon (LEU) (used to produce 1 viral suspensions) (Leucate, lat.: 43.379
160 and long.: 3.571). Seven days after SPF spat were transferred into the four locations, and as mortality
161 began to occur, oysters were brought back to the laboratory and maintained at a temperature of 20°C for
162 7 days. During this period, moribund oysters were systematically sampled daily and then stored at -
163 80°C.

164 In total, nine viral suspensions were prepared according to an established protocol (Schikorski et al.,
165 2011) (Figure 1, Table S1).

166

bioRxiv preprint doi: https://doi.org/10.1101/2025.02.07.637049; this version posted February 7, 2025. The copyright holder for this preprint (which was not certified by peer review) is the author/funder, who has granted bioRxiv a license to display the preprint in perpetuity. It is made available under aCC-BY-NC 4.0 International license.

Figure 1: Origin of samples collected to produce viral suspensions.

The samples used to produce the nine viral suspensions were collected between 2020 and 2021 from four locations: Brest harbor (red point), Marennes-Oléron basin (orange point),Arcachon bay (blue point) and Leucate lagoon (green point).

Inoculum viral load quantification and viral suspension mix setup.

To prepare an equimolar viral inoculum for injection into oysters, viral load of each of the nine viral suspension was assessed. To do so, DNA was extracted from 100 µl of each viral suspension using the MagAttract® HMW DNA kit according to manufacturer's protocol. DNA purity and concentration were assessed by Nano-Drop ND-1000 spectrometer (Thermo Scientific) and Qubit® dsDNA BR assay kits (Molecular Probes Life Technologies), respectively. Then quantification of viral copies was carried out by quantitative PCR using a Mx3005 P Thermocycler (Agilent) (Pepin et al. 2008). The outcomes were expressed as the log-transformed copy number of viral DNA per microliter of sea water (cp/µL).

The nine viral suspensions were pooled to produce the initial viral inoculum (Table S1). To account for variability in the viral copy numbers of each suspension, the pool was generated to ensure equimolarity of the viral copy numbers (Table S1).

Experimental evolution design

The EE was conducted under controlled laboratory conditions in a Type 2 laboratory at Ifremer's La Tremblade facilities. To initiate the experimental infections, 50 oysters from each oyster populations

bioRxiv preprint doi: https://doi.org/10.1101/2025.02.07.637049; this version posted February 7, 2025. The copyright holder for this preprint (which was not certified by peer review) is the author/funder, who has granted bioRxiv a license to display the preprint in perpetuity. It is made available under aCC-BY-NC 4.0 International license.

underwent prior myorelaxation using hexahydrate $MgCl_2$ (50 g/L) (Suquet et al., 2009). For each oyster population, oysters were individually injected with a 26-gauge needle attached to a multi-dispensing hand pipette. They received 100 µL of pooled inoculum into the abductor muscle (Figure 2, step 1). Simultaneously, for each oyster population, a group of 10 oysters underwent myorelaxation and were injected with artificial sea water, used as a control. The experiment was conducted in duplicate, (*i.e.* 2 batches of oysters in 2 tanks) and placed in 5 L plastic tanks filled with seawater at a temperature of 20°C and with a phytoplankton mixture (*Isochrysis galbana, Tetraselmis suecica* and *Skeletonema costatum*). Daily mortality monitoring was carried out for 7 days.

After the initial infection, nine tanks were set up: two with infected oysters and one with ASW-injected oysters for each of the three oyster populations. These nine tanks served as the starting point, referred to as "Generation 0" (Figure 2, step 2). To create the first generation of infection (G1) through cohabitation, 25 healthy oysters from each oyster population were introduced 24 hours after infecting the donor oysters (Figure 2, step 3). These healthy oysters were placed in their respective oyster population tank (i.*e.*, 25 individuals from the FA oyster population added to each FA oyster population's infection replicate, and so on). After introducing the healthy oysters to the contaminated tank, they were moved to fresh, pathogen-free seawater 24 hours later to release viral particles (Figure 2, step 4), initiating a second generation of infection. The process of adding healthy oysters and moving them for excretion was repeated for the second generation, following the same procedure as outlined above. During this period, the donor oysters from the cohabitation step were monitored for 7 days to estimate mortality rates (Figure 2, step 5), and all moribund oysters were collected for DNA extraction (see below). In total, we performed 13, 18, and 28 generations for the FA, C, and NFA oyster populations, respectively.

DNA extraction and sequencing

DNA extraction was performed on oysters collected during mortality monitoring (Figure 2, step 5) at generations G0, G5, G10, and G13 for the FA oyster population, at generations G0, G5, G10, G15, and

bioRxiv preprint doi: https://doi.org/10.1101/2025.02.07.637049; this version posted February 7, 2025. The copyright holder for this preprint (which was not certified by peer review) is the author/funder, who has granted bioRxiv a license to display the preprint in perpetuity. It is made available under aCC-BY-NC 4.0 International license.

G18 for the C oyster population, and at generations G0, G5, G10, G15, G20, G24, and G28 for the NFA oyster population. For each oyster population, infection generation, and replicate, seven samples of 35 mg of mantle tissue were collected for DNA extractions. DNA extractions were performed using the MagAttract® HMW DNA kit according to manufacturer's protocols. DNA purity and concentration were assessed with Nano-Drop ND-1000 spectrometer (Thermo Scientific) and Qubit® dsDNA BR assay kits (Molecular Probes Life Technologies), respectively. Then, quantification of viral copies was carried out by quantitative PCR using a Mx3005 P Thermocycler (Agilent), as detailed earlier. DNA samples from three individuals in each oyster population and replicate were selected based on viral load and DNA concentration. Overall, 96 samples were sequenced by DNA-seq Illumina by IntegraGen SA (Evry, France). PCR free libraries were prepared with the Twist library Preparation Enzymatic Fragmentation (EF) Kit 1.0 (Twist Bioscience) according to supplier recommendations. In brief, following a specific double strand gDNA quantification, 400ng of DNA products were processed. An enzymatic fragmentation was performed to obtain approximately 400bp inserts fragments length. After enzymatic fragmentation, end-repair, A-tailing, ligation to UDI Illumina adapters, libraries were purified and sized with SPRI beads. Sized libraries were then quantified by qPCR and sequenced on the Illumina NovaSeq sequencer as paired-end 150 bp reads.

bioRxiv preprint doi: https://doi.org/10.1101/2025.02.07.637049; this version posted February 7, 2025. The copyright holder for this preprint (which was not certified by peer review) is the author/funder, who has granted bioRxiv a license to display the preprint in perpetuity. It is made available under aCC-BY-NC 4.0 International license.

225

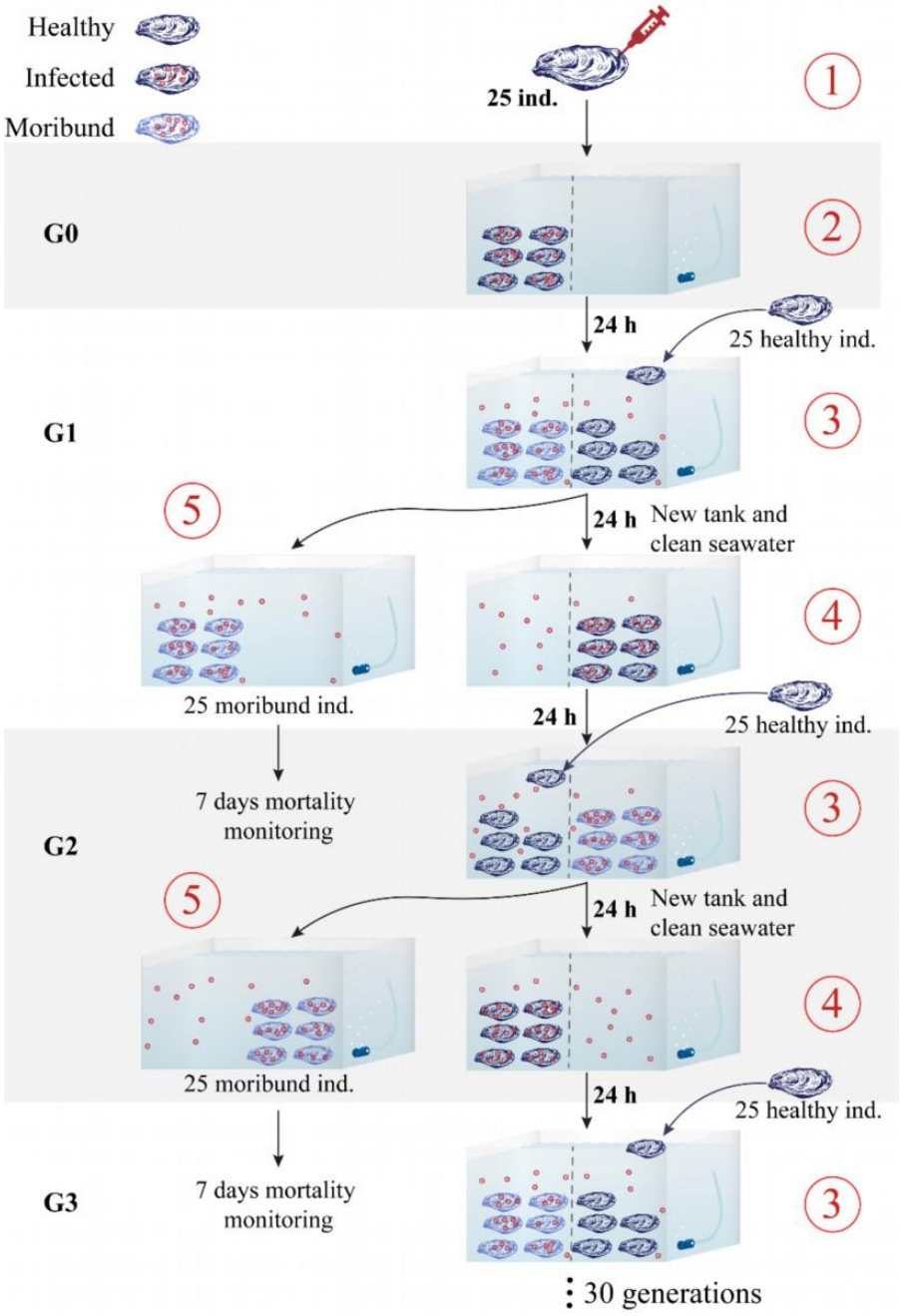

Figure 2: Experimental evolution design for one oyster population.

The experimental evolution was conducted using three oyster populations. Healthy oysters are represented in dark blue, infected oysters in dark blue with red points, and moribund oysters in light blue with red points. All experiments were performed in duplicate. The experimental steps included 1) infection of 25 healthy oysters via intramuscular injection, 2) placement of infected oysters in a tank with clean seawater to initiate viral particle production, 3) addition of 25 new healthy oysters to the tank 24 hours post-infection for exposure, 4) transfer of newly infected oysters to a new tank with clean seawater 24 hours after cohabitation to promote viral particle release, 5) counting of moribund oysters over seven days to estimate mortality rates.

226

bioRxiv preprint doi: https://doi.org/10.1101/2025.02.07.637049; this version posted February 7, 2025. The copyright holder for this preprint (which was not certified by peer review) is the author/funder, who has granted bioRxiv a license to display the preprint in perpetuity. It is made available under aCC-BY-NC 4.0 International license.

Assembly of a global consensus for each viral suspension

To obtain an overall consensus for each of the viral suspensions, viruses have been sequenced from infected oyster tissue from the same batches used for viral suspension preparation. DNA extractions, purity, concentration and quantification of viral copies were assessed as described previously (see DNA extraction and sequencing). DNA libraries were prepared using a Shotgun PCR-free library preparation kit (Lucigen) and were sequenced using Illumina NovaSeq™ 6000 device (paired-ends, 150 bp) by the Genome Quebec Company (Genome Quebec Innovation Center, McGill University, Montreal, Canada).

Raw data have been deposited in the SRA database under Bioproject PRJNA1216400 with accession numbers SAMN46433918 to SAMN46434013 for future reference and accessibility (Table S2).

De novo OsHV-1 NR-genome assemblies were obtained by processing sequenced reads as previously described (see Dotto-Maurel et al., 2022 for details on the bioinformatic pipeline).

To establish a consensus representative of the overall viral suspension used to infect oysters, we performed a multiple alignment of these 126 previously assembled genomes (Figure 3) using MAFFT v1.4.0 (Katoh et al., 2002). The consensus sequence was derived from the alignment and is composed by all the major alleles of OsHV-1 genotypes within the viral suspension. In the forthcoming sections of this manuscript, this consensus will be referred as the “artificial OsHV-1 major NR-consensus”.

bioRxiv preprint doi: https://doi.org/10.1101/2025.02.07.637049; this version posted February 7, 2025. The copyright holder for this preprint (which was not certified by peer review) is the author/funder, who has granted bioRxiv a license to display the preprint in perpetuity. It is made available under aCC-BY-NC 4.0 International license.

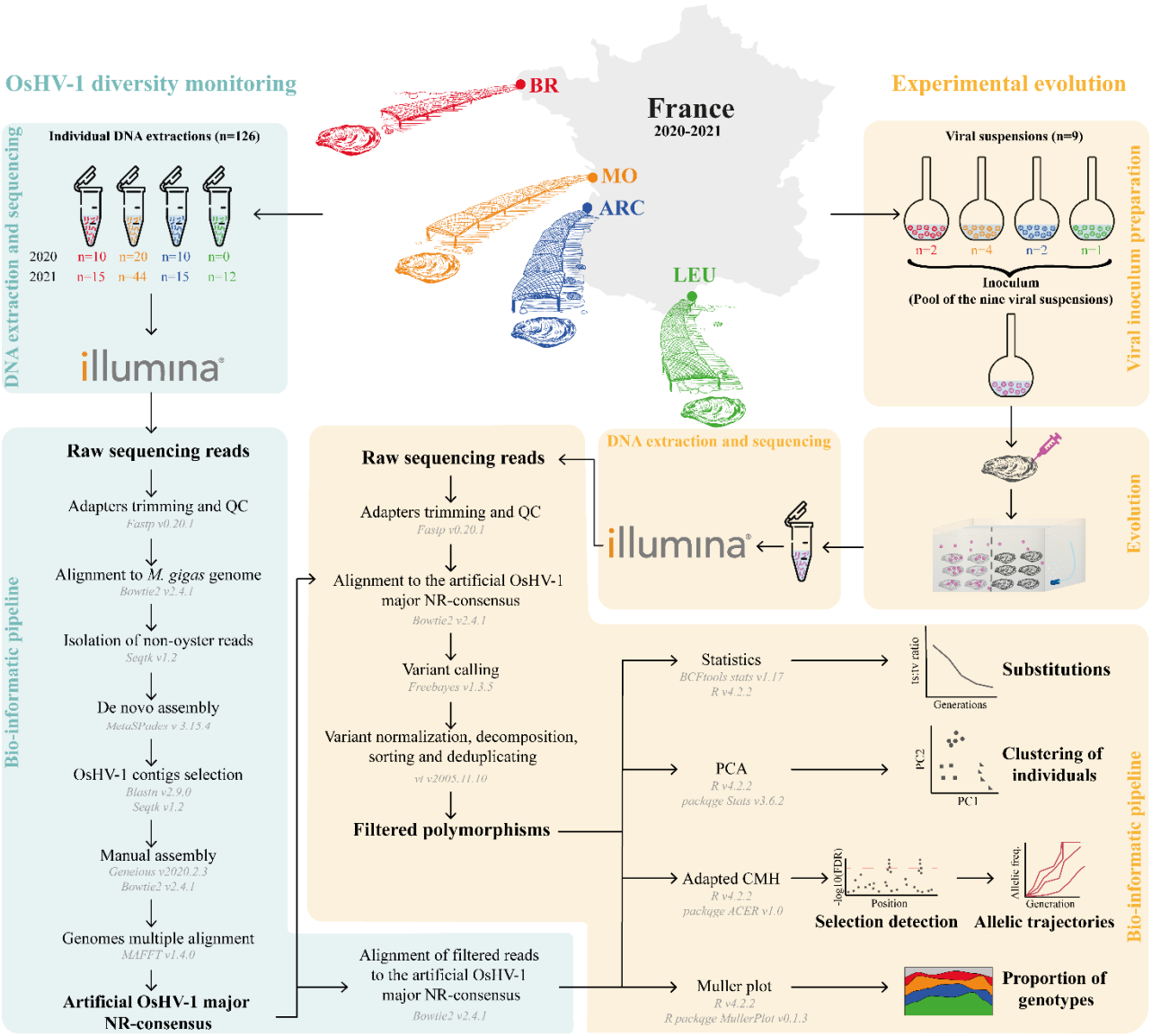

Figure 3: Bioinformatic pipeline used to analyze the dataset and detect selection patterns within OsHV-1 genomes

Steps in blue represent the monitoring of OsHV-1 diversity in France between 2020 and 2021. Pieces of mantle collected from moribund oysters were used to extract DNA, which was sequenced using Illumina technology. Raw reads were assembled *de novo* into OsHV-1 NR-genomes through a specific bioinformatic pipeline previously developed for OsHV-1 genomic analysis (Dotto-Maurel-Pelletier et al., 2019).

Steps in orange represent the analysis of experimental evolution samples and the detection of selection patterns. Moribund oysters collected between 2020 and 2021 were used to produce nine viral suspensions, which were pooled based on equimolar viral copy numbers and named “Inoculum.” Experimental evolution was conducted using this inoculum as the primary source of infection, as described in Figure 2. Pieces of mantle from moribund oysters were used to extract DNA, which was sequenced using Illumina technology. A specific bioinformatic pipeline was developed to detect and characterize traces of selection pressure.

243

bioRxiv preprint doi: https://doi.org/10.1101/2025.02.07.637049; this version posted February 7, 2025. The copyright holder for this preprint (which was not certified by peer review) is the author/funder, who has granted bioRxiv a license to display the preprint in perpetuity. It is made available under aCC-BY-NC 4.0 International license.

Variant calling

The variant calling step was performed using an adapted approach previously employed to detect polymorphisms (Figure 3, see Delmotte-Pelletier et al., 2022 for the detailed bioinformatic pipeline).

Analysis of substitutions types and clustering of individuals based on SNPs

To obtain detailed information about transitions (*i.e.* substitution of a purine by a purine or a pyrimidine by a pyrimidine) and transversions (*i.e.* substitution of a purine by a pyrimidine or a pyrimidine by a purine) number within OsHV-1 genome across generations and among host oyster populations, polymorphisms detected in all libraries were used to compute statistics with BCFtools stats v1.17 (Figure 3, Danecek et al., 2021). Substitution statistics were averaged by generation and by oyster population and were then plotted using R v4.2.2 and the ggplot package v3.4.0 (Wickham, 2009).

Exploring sample clustering and SNP data quality assessment through Principal Component Analysis

In the context of EE studies, Principal Component Analysis (PCA) is employed to assess sample clustering and evaluate the quality of Single Nucleotide Polymorphisms (SNPs) data, aiding in uncovering underlying population structure and identifying potential data anomalies (Patterson et al., 2006).

Utilizing SNP frequencies, the individuals have been projected onto a bidimensional space to check samples clustering. The PCA analysis was performed with the function pcrcomp of the factoextra v1.0.7 package (Kassambara & Mundt, 2020) in R v4.2.2 (Figure 3). This information was linked to those of oyster populations, infection generation and replicates.

bioRxiv preprint doi: https://doi.org/10.1101/2025.02.07.637049; this version posted February 7, 2025. The copyright holder for this preprint (which was not certified by peer review) is the author/funder, who has granted bioRxiv a license to display the preprint in perpetuity. It is made available under aCC-BY-NC 4.0 International license.

Selection detection

Selection patterns were detected using a SNP-based method. As the experiment was performed in duplicates for three oyster populations, selected SNPs could be detected within each oyster population in all replicates or in specific replicates. Selection of particular OsHV-1 genotypes within the different oyster populations is independent, and detected SNPs were not comparable among oyster populations. Consequently, analyses were carried out for each oyster population independently. Initially, to identify SNPs demonstrating significant shifts in allele frequency (AF), a comparison was made between the initial (G0) and evolved populations (reaching G13, G18, and G28 for FA, C and NFA oyster populations, respectively). To achieve this, an adapted Cochran-Mantel-Haenszel (CMH) test was used (Figure 3), which calculated p-values for each SNP detected within the datasets using the ACER v1.0 package (Barghi et al., 2020; Spitzer et al., 2020) in R. These p-values reflect the variance in SNP frequencies across generations while accounting for the influences of genetic drift and sampling (Spitzer et al., 2020). Subsequent to this, the p-values underwent adjustment using the false discovery rate (FDR) method, as implemented in the p.adjust function from the stats v4.2.2 package (R Development Core Team, 2005). The resultant adjusted p-values were then plotted onto the OsHV-1 genome using a Manhattan plot, using the ggplot2 v3.4.0 package (Wickham, 2009). Alleles were considered as under selection when p-values were higher than the CMH cutoff determined as 5% of false discovery rate. Finally, using the adjusted p-values and the allelic frequencies of SNPs across generations, allelic frequency trajectories were generated for each replicate. This visualization was achieved using the ggplot v3.4.0 package (Wickham, 2009).

Genotypes proportions

A Muller plot was used to visualize the emergence or loss of genotypes specific to the origin of the initial viral suspension used to infect the oysters. As described previously, the initial viral suspension injected into oysters at G0 was produced by pooling of nine viral suspensions. Libraries associated with the sequencing of the individuals collected during the same mortality events within each basin were used to determined SNPs specific to each origin. Raw reads were then filtered and trimmed as described

bioRxiv preprint doi: https://doi.org/10.1101/2025.02.07.637049; this version posted February 7, 2025. The copyright holder for this preprint (which was not certified by peer review) is the author/funder, who has granted bioRxiv a license to display the preprint in perpetuity. It is made available under aCC-BY-NC 4.0 International license.

293 previously, and aligned to the "artificial OsHV-1 major NR-consensus". Variant were called using
294 Freebayes and named using unique identifier as described above (Figure 3).

295 Each sample was collected from a specific location, allowing each SNP detected in the libraries to be
296 assigned accordingly. SNPs identified during the EE of OsHV-1 were classified by their origin and used
297 to visualize their relative abundance within each origin using the MullerPlot package v0.13 (Farahpour
298 et al., 2022) in R (Figure 3).

299

300 # Results

301 ## Evolution of survival rates and viral load in Pacific Oyster spat infected with OsHV-1 across
302 generations

303 To assess the impact of the infection by the pool of OsHV-1 genotypes on Pacific oyster spat, the
304 survival rate was monitored for 7 days post-infection (dpi) in both infected replicates and control tanks
305 for each of the three oyster populations. No oyster mortality was observed in the conditions without
306 viral infection (*i.e.* ASW-injected oysters) throughout the entire experiment.

307 Cohabitation-induced infection relies on viral propagation within the host. Challenges in sustaining
308 reinfection through successive generations led to the termination of experimental evolution at the 13th
309 generation for the farming area (FA) population, the 18th for the control (C) population, and the 28th for
310 the non-farming area (NFA) population.

311 Mortality rates fluctuated across generations but showed an overall decline over the course of
312 experiment (Figure 4A). At G0, mortality rates were 88%, 96%, and 84% respectively for FA, C and
313 NFA oyster populations. In the C population, mortality steadily decreased to 42% at G15 before rising
314 to 56% at G18, at which point the experiment ended due to the absence of mortality at G19.

315 In contrast, FA and NFA populations showed variable mortality trends. FA oysters experienced a sharp
316 drop of mortalities to 58% at G5, a rise to 87% at G10, and a drastic decline to 2% thereafter, leading to

bioRxiv preprint doi: https://doi.org/10.1101/2025.02.07.637049; this version posted February 7, 2025. The copyright holder for this preprint (which was not certified by peer review) is the author/funder, who has granted bioRxiv a license to display the preprint in perpetuity. It is made available under aCC-BY-NC 4.0 International license.

317 experiment termination. NFA oysters followed a similar pattern beginning with a decrease of mortalities
318 to 50% at G5, a spike to 99% mortality at G10, then fluctuations between 28% and 89% mortality.

319 Variations in viral loads were observed both among individuals and among oyster populations (Figure
320 4B). The mean viral load within individuals from the oyster populations FA exhibited a slight increase
321 across generations, rising from $8.38x10^5 \pm 5.49x10^5$ viral DNA copies/ng of DNA at G0 to $1.13x10^6 \pm$
322 $4.81x10^5$ viral DNA copies/ng of DNA (Figure 4B). Conversely, the average viral load within
323 individuals from the oyster populations C and NFA demonstrated a slight decrease across generations.
324 For the population C, the viral load varied from $6.62x10^5 \pm 4.49x10^5$ viral DNA copies/ng of DNA at
325 G0 to $3.34x10^5 \pm 2.54x10^5$ viral DNA copies/ng of DNA at G18. In the case of the population NFA, the
326 viral load ranged from $2.09x10^6 \pm 1.20x10^6$ viral DNA copies/ng of DNA at G0 to $9.35x10^5 \pm 1.11x10^6$
327 viral DNA copies/ng of DNA at G28 (Figure 4B).

328

329

bioRxiv preprint doi: https://doi.org/10.1101/2025.02.07.637049; this version posted February 7, 2025. The copyright holder for this preprint (which was not certified by peer review) is the author/funder, who has granted bioRxiv a license to display the preprint in perpetuity. It is made available under aCC-BY-NC 4.0 International license.

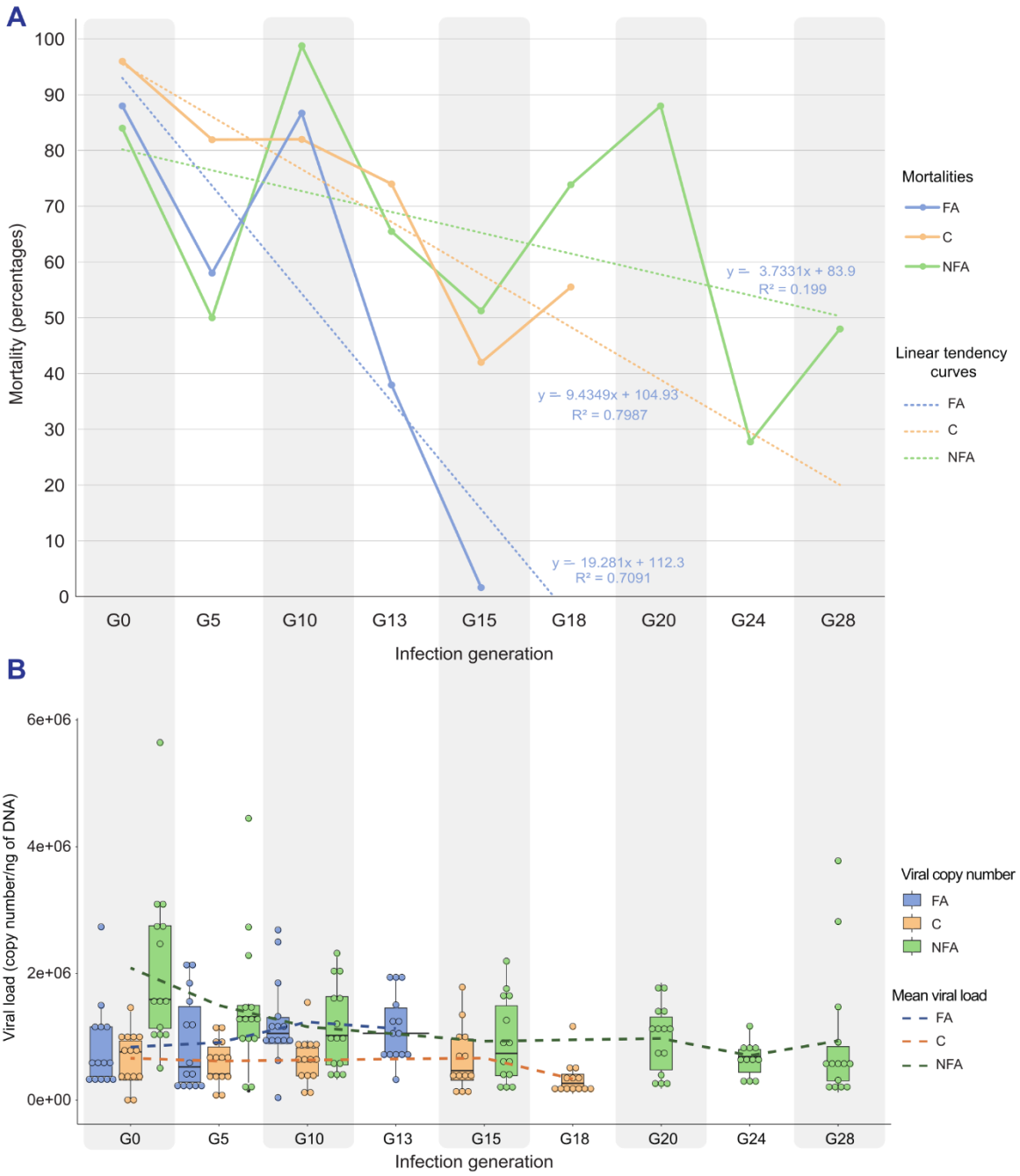

Figure 4: Oyster mortalities and viral load from the three oyster populations at generations 0, 5, 10, 13, 15, 18, 20, 24 and 28.

A) Oyster mortality was monitored daily to estimate mortality rates within each oyster population for selected generations. The solid curves and dotted lines correspond to mortality rates and the linear tendency of mortality rates respectively, for oysters from the line FA oyster population (in blue), from the C oyster population (in orange), and from the NFA oyster population (in green).

B) Viral loads were assessed from seven individuals for each generation, oyster population, and replicate to monitor the evolution of the infection over generations. Viral loads of individuals are represented by points (in blue, orange, and green for oysters from lines FA, C, and NFA, respectively). The box plots represent median values, the first and third quartiles, and the standard deviation of viral loads within an oyster population for a specific generation. The dotted lines illustrate the viral load for oysters from the FA oyster population (in blue), from the C oyster population (in orange), and from the NFA oyster population (in green).

330

bioRxiv preprint doi: https://doi.org/10.1101/2025.02.07.637049; this version posted February 7, 2025. The copyright holder for this preprint (which was not certified by peer review) is the author/funder, who has granted bioRxiv a license to display the preprint in perpetuity. It is made available under aCC-BY-NC 4.0 International license.

Dynamics of substitutions and transition / transversion ratio

Studying substitution patterns across viral generations in EE is crucial for understanding evolutionary dynamics, genetic diversity, and adaptation (Bromham, 2020).

A prominent trend emerges for all three oyster populations, indicating a rapid reduction in the count of SNPs in the OsHV-1 genome across the populations throughout the generations of infection (Figure 5). The trend is more pronounced for the NFA oyster population extending from 372 ± 55 SNPs at G0 to 294 ± 43 SNPs at G5 (Figure 5A).

A statistical analysis, based on the identified SNPs, was conducted to assess the transition / transversion (ts/tv) bias (Figure 5B). The ts/tv ratio of the virus remained consistently below 1 across all generations and lines, except for the samples collected from the FA oyster populations at G0, for which the virus displayed a ts/tv ratio of 1.26, indicating an excess of transitions (Figure 5B). Additionally, the viral ts/tv ratio demonstrates a decreasing trend over generations for both the FA and C oyster populations. Regarding the NFA oyster populations, the overarching pattern leans towards a decline in the ts/tv ratio; however, an upward shift in the ratio is noticeable in G10.

bioRxiv preprint doi: https://doi.org/10.1101/2025.02.07.637049; this version posted February 7, 2025. The copyright holder for this preprint (which was not certified by peer review) is the author/funder, who has granted bioRxiv a license to display the preprint in perpetuity. It is made available under aCC-BY-NC 4.0 International license.

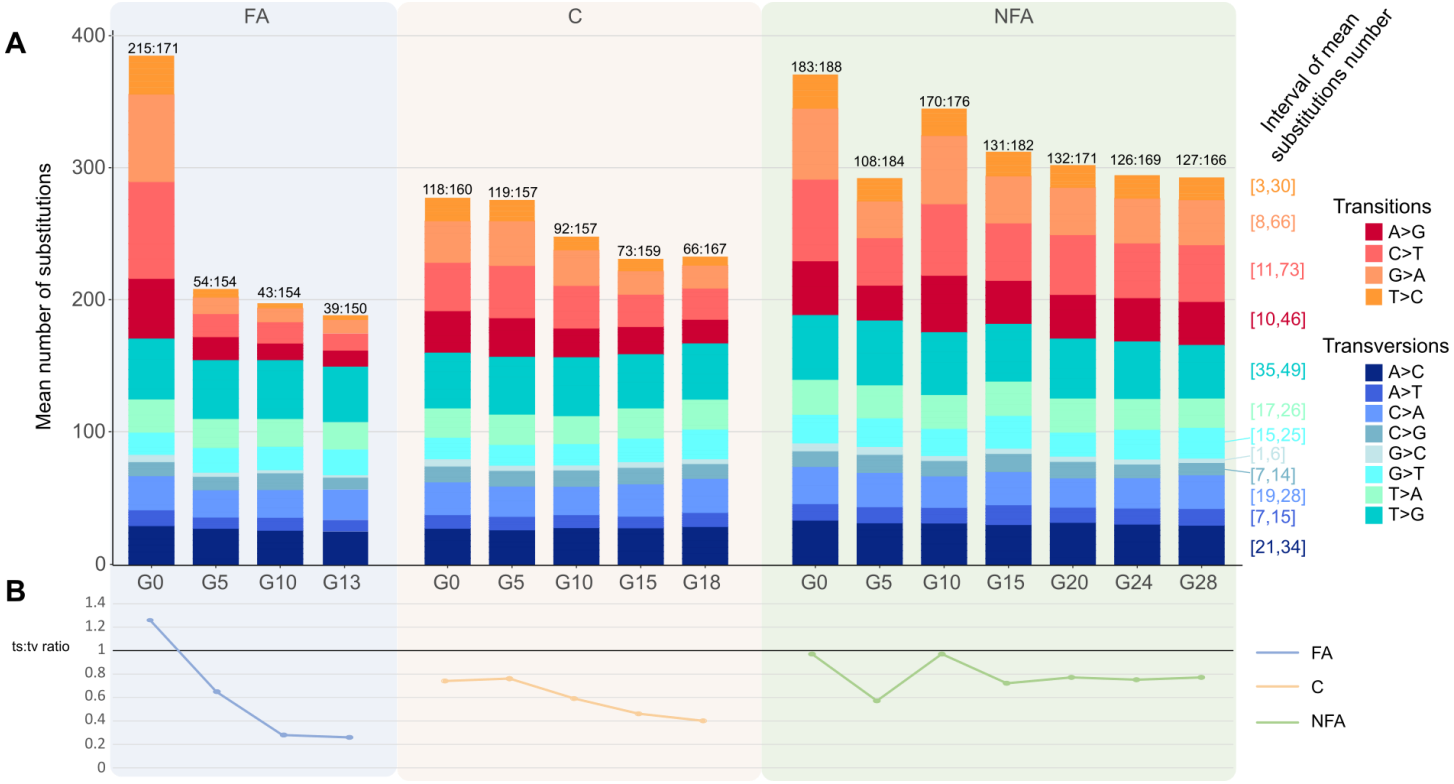

Figure 5 : Substitution types and transition:transversion ratio observed within OsHV-1 populations.

A) The mean number of viral substitution types per generation and oyster population is shown. Transitions (substitutions of a pyrimidine by a pyrimidine or a purine by a purine) are represented by a gradient from red to orange, while transversions (substitutions of a purine by a pyrimidine or vice versa) are shown with a gradient from blue to green. The numbers above the stacked bars indicate the counts of transitions and transversions, while the numbers in square brackets to the right of the bars represent the average number of each substitution type in the samples.

B) Curves illustrating variations in the ts:tv ratio across generations for each oyster population. Line colors correspond to the different oyster populations.

Unveiling OsHV-1 population structure and anomalies in experimental evolution through SNP Data analysis and principal component projection

Using SNP frequencies, we projected individuals OsHV-1 genomes onto a bidimensional space (Figure 6). The first principal component axis accounted for 12.61% of the variance in the data, while the second principal component axis explains 9.89% of the variance (Figure 6). The first principal component aligns with the progression of infection generations, while the second component is indicative of oyster population associations or susceptibility traits within oyster populations. The graphical representation reveals the presence of four distinct clusters corresponding to the interplay between oyster populations and infection generations.

bioRxiv preprint doi: https://doi.org/10.1101/2025.02.07.637049; this version posted February 7, 2025. The copyright holder for this preprint (which was not certified by peer review) is the author/funder, who has granted bioRxiv a license to display the preprint in perpetuity. It is made available under aCC-BY-NC 4.0 International license.

The first cluster encompasses samples from all oyster populations at G0, with those collected from the replicate 1 of the C population at G0, G5, G10, G15, and G18 (Figure 6A, group 1) suggesting a maintenance of the initial diversity along the generation 0 to 18 in the replicate 1 of the C population.

The second cluster (Figure 6A, group 2) encompasses samples primarily collected from FA line at G5, G10, and G13, as well as the replicate 2 from C line at G5, G10, G15, and G18.

Finally, the third cluster comprises specimens sourced from the NFA oyster population, further divided into two subsets. The initial subset (Figure 6A, group 3.1) exclusively represents samples obtained during G5, while the second subset (Figure 6A, group 3.2) corresponds to samples collected between G15 and G28.

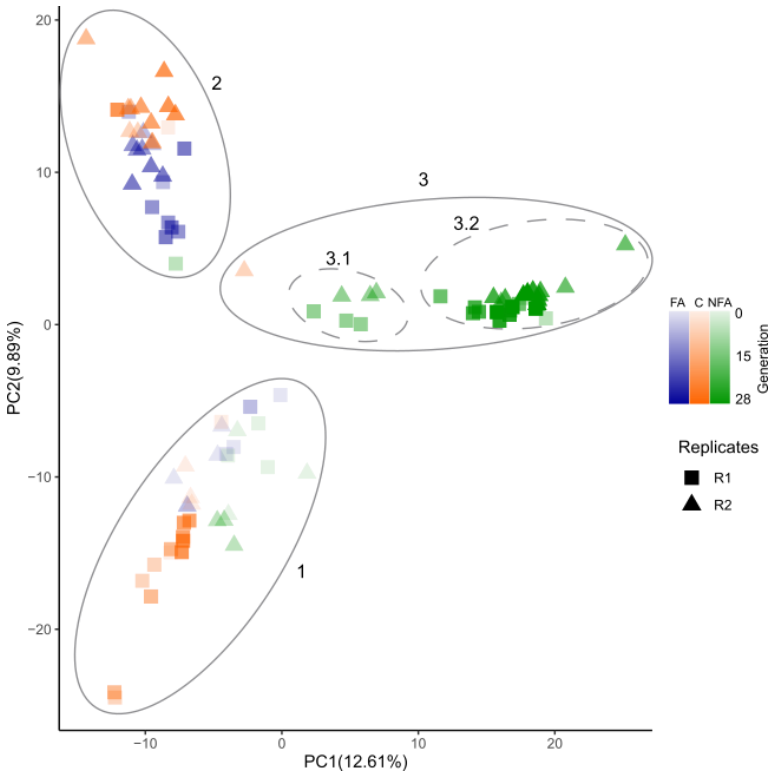

Figure 6 : Principal component analysis reveals OsHV-1 population structure and generation-oyster populations associations.

Projection of individual similarities onto the first and second principal components. The colors of the points correspond to the infected oyster populations: individuals from the FA oyster population are colored in blue, individuals from the C oyster population are colored in orange, and individuals from the NFA oyster population are colored in green. Infection generations are represented by a gradient of colors, and replicates are indicated by different point types (square for replicate 1 and triangle for replicate 2). The clustering of samples is indicated by ellipses and numbered from 1 to 3. For the cluster 3, two subclusters were identified numbered 3.1 and 3.2.

bioRxiv preprint doi: https://doi.org/10.1101/2025.02.07.637049; this version posted February 7, 2025. The copyright holder for this preprint (which was not certified by peer review) is the author/funder, who has granted bioRxiv a license to display the preprint in perpetuity. It is made available under aCC-BY-NC 4.0 International license.

Detection of regions under selection pressure and allelic frequency trajectories

The Cochran-Mantel-Haenszel test (CMH) is widely used to detect selection pressures by analyzing allele frequency shifts in experimental evolution and time series data (Spitzer et al., 2020).

The CMH test, employed on SNPs detected within each viral population collected from the three oyster populations independently (Figure 7), revealed that in oyster populations FA (Figure 7A) and C (Figure 7B), no regions were significantly impacted by selection. However, within the NFA oyster populations, a total of 117 positions demonstrated candidate selection signatures (Figure 7C). These positions are distributed across the entire OsHV-1 genome, with a distinct emphasis on specific regions, such as repeated regions or the UL region spanning 50 kb to 80 kb. More precisely, 28 potentially selected positions were located within intergenic regions, including one SNP in the stem loop, and 89 SNPs were located within ORFs (Figure 8, Table S3).

Specifically, among the 89 SNPs situated within ORFs, 58 correspond to ORFs with undefined functions, while 12 are found within ORFs encoding transmembrane proteins (Table S3). Additionally, 8 SNPs are situated within ORFs encoding secreted proteins, four within ORF 100 coding for a DNA polymerase, three within ORFs encoding Zinc-finger, Ring-type proteins, two within ORFs encoding BIR repeat motifs, one within ORF115 associated with an Origin-binding protein, and the final SNP within ORF20 encoding a ribonucleotide reductase (Table S3).

bioRxiv preprint doi: https://doi.org/10.1101/2025.02.07.637049; this version posted February 7, 2025. The copyright holder for this preprint (which was not certified by peer review) is the author/funder, who has granted bioRxiv a license to display the preprint in perpetuity. It is made available under aCC-BY-NC 4.0 International license.

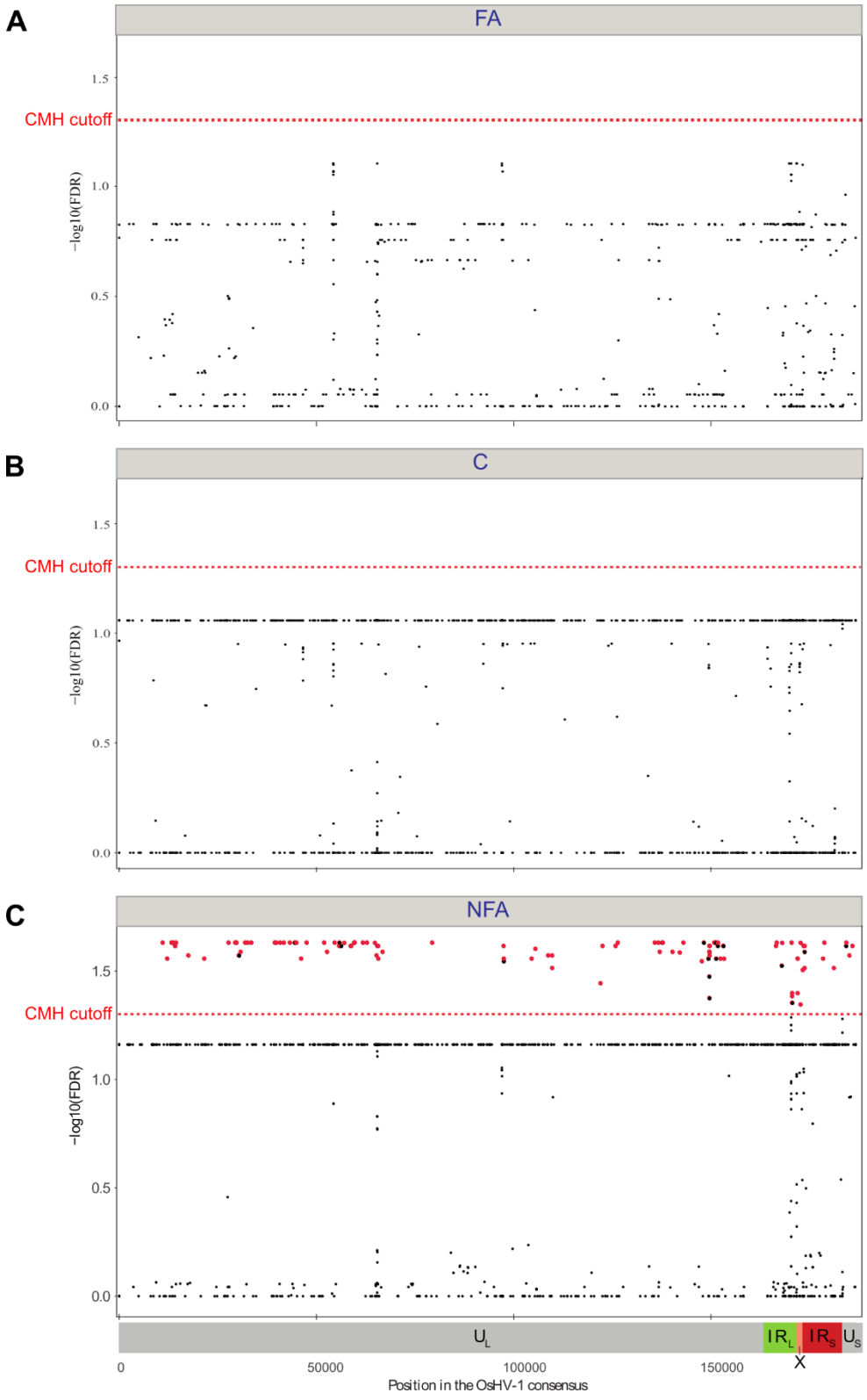

Figure 7: Genomic distribution of candidate SNPs in oyster populations.
The scatter plots show the negative log10-transformed p-values of SNPs corresponding to genomic positions for A) Farming area, B) Control and C) Non-Farming area oyster populations. These p-values were calculated using the CMH test, which involved comparing the viral populations of the founder and evolved states. Significance thresholds are indicated by red dotted lines, representing the CMH cutoff at a 5% false positive rate. Significant p-values are highlighted by red points. The genomic architecture of the OsHV-1 genome is represented below the graphs, depicting unique and repeated regions as follows: U_L/U_S (unique long/short) and IR_L/IR_S (inverted repeat long/short).

384

bioRxiv preprint doi: https://doi.org/10.1101/2025.02.07.637049; this version posted February 7, 2025. The copyright holder for this preprint (which was not certified by peer review) is the author/funder, who has granted bioRxiv a license to display the preprint in perpetuity. It is made available under aCC-BY-NC 4.0 International license.

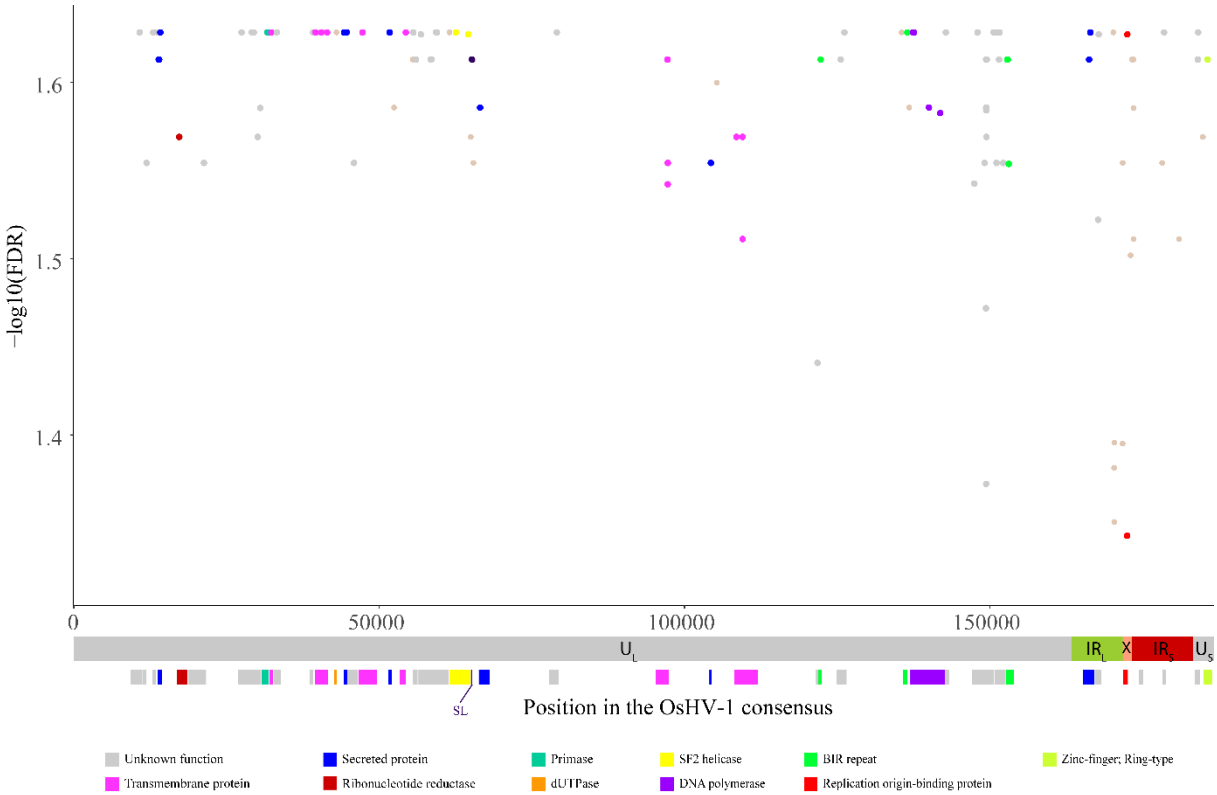

Figure 8: Zoom on the genomic distribution of selected SNPs in Non-Farming area oyster population.
The scatter plot shows the negative log10-transformed p-values of selected SNPs corresponding to genomic positions. These p-values were calculated using the CMH test, which involved comparing the viral populations of the founder and evolved states. Significance thresholds representing the CMH cutoff at a 5% false positive rate are displayed. Below the plots, the genomic structure of the OsHV-1 genome is presented, highlighting distinct segments such as unique and repeated regions denoted as U_L/U_S (unique long/short) and IR_L/IR_S (inverted repeat long/short). Moreover, the genomic architecture is supplemented by the depiction of ORFs (Open Reading Frames) housing the selected SNPs, color-coded based on their encoded functions or domains. SL: Stem-loop. The SNPs themselves are also color-coded according to the specific impact they have on the function of the corresponding ORF.

385

386 An allelic frequency trajectories (AFT) plot was employed for candidate SNPs detected within the NFA
387 oyster population to track changes in allelic frequencies over generations and get insights into the
388 evolutionary dynamics within populations, especially for positive selection (Barghi et al., 2020). The
389 analysis of allelic frequency trajectories has been performed separately for both replicates (Figure 9).

390 The AFT plot of candidate SNPs reveals a general trend of increasing allelic frequencies, ultimately
391 resulting in the fixation of selected alleles in both replicates. However, in the first replicate, the allelic
392 frequencies of candidate SNPs increase between G0 and G5, then decrease between G5 and G10, and
393 finally increase again between G10 and G15 to reach fixation (Figure 9A). In the second replicate, a
394 similar trend is observed, but only for 77 SNPs (Figure 9B). Moreover, alleles of 66 SNPS for replicate

bioRxiv preprint doi: https://doi.org/10.1101/2025.02.07.637049; this version posted February 7, 2025. The copyright holder for this preprint (which was not certified by peer review) is the author/funder, who has granted bioRxiv a license to display the preprint in perpetuity. It is made available under aCC-BY-NC 4.0 International license.

1 and 26 SNPs for replicate 2, represented at the bottom of the plot, show an increase in frequencies, albeit to a lesser extent (Figure 9A and B).

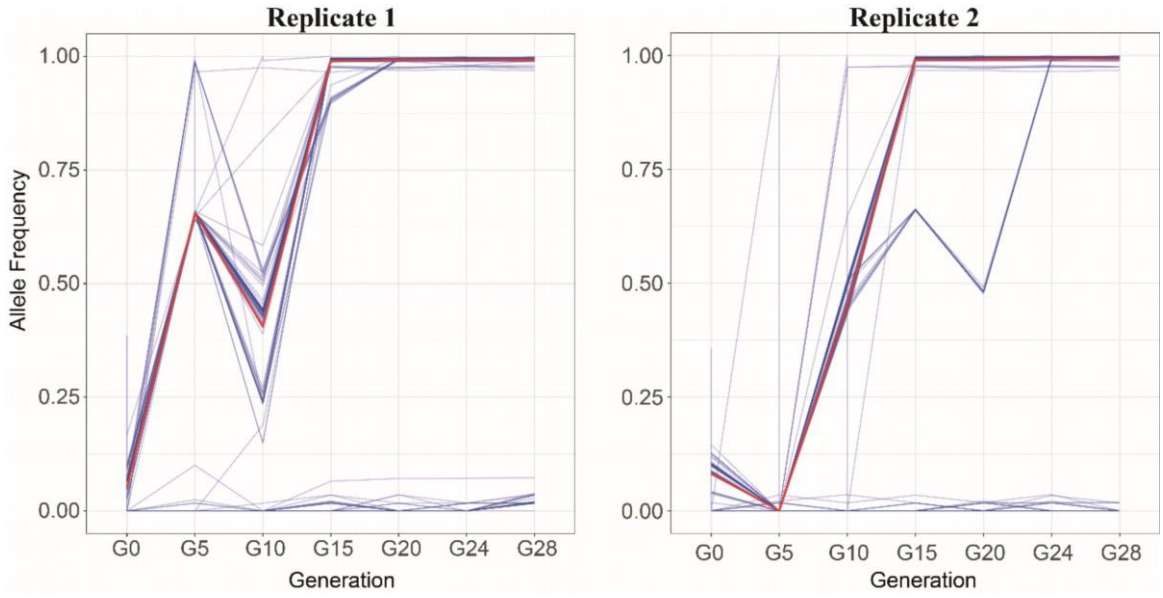

Figure 9:Allelic frequency trajectories plot for the top 100 candidate SNPs detected within the OsHV-1 samples of replicate 1 and 2 collected from oysters of the NFA oyster population.

Each blue line represents the allelic frequency trajectory of a specific SNP across generations. Red line represents the median allelic frequency trajectory.

Relative abundance of SNP from specific origin

To track the presence of viral genotypes specific to one of the geographic origins and their fate across generations of infection, a Muller plot was generated (Figure 10). The results revealed that multiple genotypes from different origins coexist from the beginning to the end of the experiment within each oyster populations. At the generation 0, the relative abundance (RA) of genotypes specific to MO and LEU is higher than that of genotypes specific to ARC and BR.

This trend is generally maintained across generations of infections for all oyster populations. However, depending on the oyster populations, the RA varies over the generations. Specifically, for the FA oyster population, OsHV-1 SNPs specific to MO are present at a RA of 0.2 in G0, then their RA increases to reach 40% in G10 before slightly decreasing. The trend is generally similar for OsHV-1 SNPs specific

bioRxiv preprint doi: https://doi.org/10.1101/2025.02.07.637049; this version posted February 7, 2025. The copyright holder for this preprint (which was not certified by peer review) is the author/funder, who has granted bioRxiv a license to display the preprint in perpetuity. It is made available under aCC-BY-NC 4.0 International license.

to ARC and BR, but with much lower RA (between 0.02 and 2.0). As for OsHV-1 SNPs specifically from LEU, the trend is reversed. Indeed, the initial RA decreased from 0.4, to 0,1 at G5.

Moreover, over the course of the experiment, SNPs that were not initially present in any of the viral suspensions began to emerge. At G0, the RA of these SNPs was relatively low within farming and non-farming oyster populations (RA = 0.1). However, as the infection generations progressed, their RA increased. In contrast, the RA of "other" SNPs within the control oyster populations at the beginning of the experiment was 0.3, and then it experienced fluctuations across generations. First, it decreased to RA=0.2 until G5, then increased to RA=0.5 until G10 and decreased to RA=0.2 until G15.

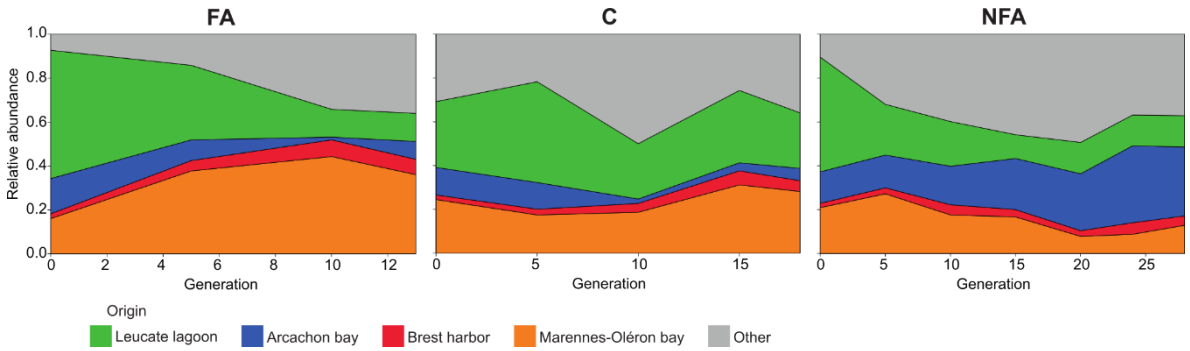

Figure 10 : Muller plot representing the relative abundance of viral SNPs collected from specific origins for each oyster population during the experimental evolution.

The relative abundance of viral SNPs is color-coded according to their geographical origin of the viral suspension: the orange area corresponds to genotypes collected specifically in MO, the red area corresponds to genotypes collected specifically in BR, the blue area corresponds to genotypes collected specifically in ARC, the green area corresponds to genotypes collected specifically in LEU, and the grey area corresponds to genotypes that appeared during the experimental evolution.

Discussion

To mitigate the impact of infectious diseases, it is essential to unravel the mechanisms that shape the evolution and dissemination of disease-causing microorganisms (Gu et al., 2021; NIH, 2007). Variability in host resistance levels is known to play a significant role in driving these processes (Gandon & Michalakis, 2000; Kubinak & Potts, 2013). This study provides valuable insights into the intricate evolutionary dynamics of OsHV-1 and its interactions with Pacific oysters, focusing on how the virus adapts and diversifies in response to variations in host genetic backgrounds. These findings shed light

bioRxiv preprint doi: https://doi.org/10.1101/2025.02.07.637049; this version posted February 7, 2025. The copyright holder for this preprint (which was not certified by peer review) is the author/funder, who has granted bioRxiv a license to display the preprint in perpetuity. It is made available under aCC-BY-NC 4.0 International license.

425 into mechanisms driving viral evolution, a crucial step in understanding and addressing the devastating
426 effects of this virus inducing POMS on the oyster farming industry.

427 During this experimental evolution, we observed a decrease in both oyster mortalities and viral load
428 across successive generations of OsHV-1 infection. This decline in mortality rates can be attributed to
429 several factors.

430 First and foremost, it can be explained by the selection of less virulent viral variants. As is well-
431 established, the interactions between a pathogen and its host are characterized by a delicate balance
432 between virulence and transmission (Anderson & May, 1982). In conditions where the oyster population
433 is limited, such as in our experimental setup with 25 individuals per tank, infected hosts succumb
434 rapidly. A plausible strategy adopted by the virus may be to reduce its virulence in order to maintain a
435 stable host population while ensuring efficient replication without lethality. It is a well-documented
436 phenomenon that there is a trade-off between virulence and transmission, where increased transmission
437 is associated with decreased virulence, and conversely, increased virulence leads to decreased
438 transmission (Anderson & May, 1982; Gandon & Michalakis, 2000; Kun et al., 2023). Similar results
439 were obtained in an EE study involving tobacco and pepper plants infected with the tobacco etch
440 potyvirus (TEV). In this study, viral load and virulence significantly decreased across generations, a
441 phenomenon linked to the host lineage, which plays a pivotal role in shaping the fate of viruses (Cuevas
442 et al., 2015).

443 Secondly, the reduction in mortality rates can be attributed to a lack of complementation between
444 genotypes (Froissart et al., 2004; Montville et al., 2005). In fact, host infection rarely occurs with a
445 single genotype, but often involves co-infection, with multiple viral genotypes contributing to the
446 infection and associated symptoms. It has already been shown that certain genotypes that have
447 developed disadvantageous mutations in important genes, can be complemented by other genotypes that
448 do not carry these mutations and whose corresponding proteins remain functional (Froissart et al., 2004;
449 Montville et al., 2005). This mechanism allows low-fitness genotypes to gain a phenotypic advantage
450 by utilizing intracellular proteins produced by co-infecting high-fitness strains (Froissart et al., 2004;
451 Montville et al., 2005). In the context of our study, where genetic diversity has likely been drastically

bioRxiv preprint doi: https://doi.org/10.1101/2025.02.07.637049; this version posted February 7, 2025. The copyright holder for this preprint (which was not certified by peer review) is the author/funder, who has granted bioRxiv a license to display the preprint in perpetuity. It is made available under aCC-BY-NC 4.0 International license.

reduced, possibly due to a bottleneck effect, it is possible that some genotypes have been purged from the viral population, leading to limited complementation events and consequently a reduction in virulence over successive generations. Bottlenecks, which occur when a population undergoes a sharp reduction in size due to factors such as transmission events or selective sweeps, can drastically reduce genetic diversity by eliminating rare variants and fixing certain alleles through genetic drift (Zwart & Elena, 2015). In viral populations, this can be particularly impactful, as beneficial interactions between co-infecting genotypes rely on the presence of genetic diversity (Zwart & Elena, 2015). If only a small subset of the original population survives a bottleneck, previously co-existing genotypes that enabled complementation may be lost, preventing the recovery of deleterious mutations and diminishing overall viral fitness (Zwart & Elena, 2015). As a result, the ability of the virus to sustain high virulence through cooperative interactions is compromised, leading to an overall reduction in mortality rates.

A third hypothesis to explain declines in mortality rates and viral loads is the temporal shift in the peak of viral particle release into seawater as infection generations progress. Consequently, the viral load would be high when cohabitation begins and progressively decreasing over time. In the case of OsHV-1, the excretion peak by oysters occurs between 24 and 48 hours post-infection (hpi) (Delmotte et al., 2020), but this timing can vary depending on several factors, including oyster susceptibility, the initial viral load in infected oysters, the number of donors, food availability, oyster age, water temperature, and salinity (Dégremont, 2011; Delmotte et al., 2020; Evans et al., 2017; Pernet et al., 2018, 2018; Petton et al., 2015; Schikorski et al., 2011). In our experiment, oysters used for successive infections came from the same cohort, meaning they aged between the start and end of the experimental evolution, potentially altering their susceptibility to infection and the timing of peak viral excretion. Additionally, previous studies have shown that oyster infections via cohabitation lead to fewer fatalities due to a progressive decline in the initial viral load from one infection cycle to the next (Cain et al., 2021). While it may not be the optimal method for EE, successive infection by cohabitation was chosen to mimic the natural infection of oysters by OsHV-1 in the field.

Genetic mutations play a pivotal role in shaping the evolutionary landscape of organisms, with transitions and transversions representing two distinct classes of point mutations that contribute to

bioRxiv preprint doi: https://doi.org/10.1101/2025.02.07.637049; this version posted February 7, 2025. The copyright holder for this preprint (which was not certified by peer review) is the author/funder, who has granted bioRxiv a license to display the preprint in perpetuity. It is made available under aCC-BY-NC 4.0 International license.

479 genetic diversity and adaptation. Molecular evolutionary hypothesis suggests that natural selection
480 promotes amino acid substitutions mostly through transitions (Stoltzfus & Norris, 2016). The substantial
481 decline in the count of single nucleotide polymorphisms (SNPs) and the decrease in the
482 transition/transversion (ts/tv) ratio across all three oyster populations over successive infection
483 generations suggest a trend toward genetic homogenization within the viral populations. This trend could
484 arise from selection favoring specific viral genotypes or from a reduction in genetic diversity due to
485 population bottlenecks (McCrone & Lauring, 2018). Interestingly, similar patterns of reduction in viral
486 variants have been observed in two distinct EE studies. Firstly, in the case of the Cucumber mosaic virus
487 injected into tobacco plants during an experimental infection, viral populations underwent a population
488 bottleneck due to genetic drift, resulting in a significant reduction in viral diversity (Li & Roossinck,
489 2004). Similarly, when Potato virus Y passed through three different potato plant genotypes with varying
490 levels of susceptibility to the virus, a combination of strong selective sweeps and bottlenecks led to a
491 reduced viral diversity by the fifth generation (Kutnjak et al., 2017). Given the context of OsHV-1
492 infecting different oyster genetic backgrounds and considering host population size, it is plausible that
493 the viral population underwent a bottleneck, leading to a reduction in the number of viral variants.

494 In contrast to the experimental developments carried out on herpesviruses, no structural variation was
495 observed in the genomes of OsHV-1 (Fuandila et al., 2022). The absence of structural variations during
496 short-term experimental evolution studies of viruses can be attributed to the limited timeframe, which
497 may be insufficient for such large-scale genomic changes to emerge or become detectable. Structural
498 variations, including large-scale rearrangements or duplications, often require extended periods to
499 develop and reach appreciable frequencies within viral populations. For instance, studies on RNA
500 viruses have demonstrated that while point mutations can accumulate rapidly, more substantial genomic
501 alterations necessitate longer evolutionary timescales (Duffy et al., 2008; Elena & Lenski, 1997).

502 The PCA analysis of SNP frequencies unveiled distinct clusters that corresponded to the different oyster
503 populations and infection generations, signifying genetic differentiation. Through the process of
504 experimental evolution, viral populations exhibited adaptability across successive generations of
505 infection, with individuals organizing into clusters according to their infection histories. Particularly

bioRxiv preprint doi: https://doi.org/10.1101/2025.02.07.637049; this version posted February 7, 2025. The copyright holder for this preprint (which was not certified by peer review) is the author/funder, who has granted bioRxiv a license to display the preprint in perpetuity. It is made available under aCC-BY-NC 4.0 International license.

noteworthy, the clustering of individuals from the non-farming (NFA) and farming area (FA) oyster populations is clearly delineated and distinct, indicating a contrasting evolution within these two populations. In contrast, control oyster population (C) exhibited mixed clustering, likely owing to their intermediate genetic status. These findings strongly suggest ongoing genetic differentiation, which could be attributed to varying levels of oysters susceptibility to OsHV-1 infection (Kubinak & Potts, 2013). Within the NFA oyster population, distinct clusters emerged, indicating evolutionary changes across infection generations in response to selective pressures.

The identification of 117 candidate selection signatures in the OsHV-1 genomes, in conjunction with the allelic frequency trajectories (AFT) plots collected from the NFA oyster population, provides compelling evidence of selective pressures acting on OsHV-1 during the course of the experimental evolution. The trend toward increasing allelic frequencies, ultimately leading to allele fixation in both replicates, strongly indicates positive selection (Barghi et al., 2020). Notably, selective pressure was exclusively detected within the OsHV-1 genome during successive infection in the NFA oyster population.

One plausible hypothesis to explain this observation is that in more susceptible oysters, viral replication is favored (Dégremont, 2011), leading to an increase in mutation rates and enabling the fixation of advantageous alleles within populations (Elena & Sanjuán, 2005; Peck & Lauring, 2018). Given that viral diversity and natural selection processes in viruses are primarily influenced by environmental changes or by the host's immune system acting as a filter to limit viral diversity and adaptation, one might have expected to detect selection signals in viral genomes infecting the FA oyster population (Kubinak & Potts, 2013). However, since no selection signals were detected for the FA oyster population, despite the observed reduction in viral diversity, this strengthens the hypothesis that the viral populations infecting the FA oyster population may have been influenced by a bottleneck effect and genetic drift.

These selection signatures are distributed across the viral genome, with a specific emphasis on repetitive segments and the U_L region. The presence of selection signatures within ORFs encoding various proteins suggests that both regulatory and functional elements of the virus are under selective pressure.

bioRxiv preprint doi: https://doi.org/10.1101/2025.02.07.637049; this version posted February 7, 2025. The copyright holder for this preprint (which was not certified by peer review) is the author/funder, who has granted bioRxiv a license to display the preprint in perpetuity. It is made available under aCC-BY-NC 4.0 International license.

Specifically, regions responsible for vital biological functions or domains related to the attachment of viral particles to host cells, DNA replication, synthesis, packaging, as well as transmembrane and membrane proteins, could be crucial for the adaptation to resistant or susceptible hosts. It is worth noting that viral entry proteins play a pivotal role in enhancing viral fitness, and even a single amino acid mutation within these proteins can modify the virus's ability to infect hosts with varying levels of susceptibility to infection (van Sluijs et al., 2017). Moreover, studies have revealed that various domains, including envelope domains (such as membrane glycoproteins and transmembrane receptors), auxiliary domains (like Zinc-finger, RING type, dinucleoside kinase), and modulation and control domains (such as Interleukin, Interferon-regulatory factor, or Zinc-finger), have been acquired, duplicated, or lost during the evolution of Herpesviridae (Brito & Pinney, 2020). Many of these acquired domains enabled viruses to specifically bind to host cells and to evade or manipulate the host's immune system. In the present study, the majority of the signals of selection were identified within these domains, indicating a potential adaptation of essential proteins that leads to a specialization of viral genotypes to their respective host genetic background. Additionally, two previous studies conducted on OsHV-1 (Delmotte et al., 2020; Pelletier et al., 2023) have demonstrated that selective pressure plays a key role in the adaptation of the virus to different host species and environments through mutations, particularly in ORFs encoding viral membrane-related and metabolic-related proteins, further supporting the hypothesis of immune selection of OsHV-1 within the NFA oyster population. Based on the results obtained in this study, it is evident that adaptation can also occur at a finer scale within the host's genetic background, which is influenced in this case by the geographic origin of the parental individuals (*i.e.* farmed or not farmed area).

Conclusion

This study provides valuable insights into the evolutionary forcing mechanisms of OsHV-1 and its interactions with Pacific oysters, with a particular emphasis on viral adaptation and diversification in response to host infection susceptibility. Employing an EE approach, it sheds light on the dynamic nature of host-virus interactions, the potential for viral adaptation, and the potential role of genetic diversity in shaping the outcome of these interactions. The nucleotide evolution of OsHV-1, particularly a decrease

bioRxiv preprint doi: https://doi.org/10.1101/2025.02.07.637049; this version posted February 7, 2025. The copyright holder for this preprint (which was not certified by peer review) is the author/funder, who has granted bioRxiv a license to display the preprint in perpetuity. It is made available under aCC-BY-NC 4.0 International license.

in transition and transversion numbers, appears to be mainly driven by both genetic drift and positive selection linked to the oyster genetic background, resulting in a reduction in viral diversity and the fixation of specific alleles within ORFs dedicated to host-virus interactions and virus functional maintenance. Further research into the functional consequences of these changes is necessary. These findings contribute to our understanding of the mechanisms governing viral evolution and hold significant implications for mitigating the devastating impacts of OsHV-1 on oyster farming industries. Future studies should continue to explore the intricate dynamics of host-virus interactions and their implications for viral evolution and disease management.

Data availability

Raw data have been deposited on the SRA database under Bioproject PRJNA1216400 accession numbers SAMN46433918 to SAMN46434013 for future reference and accessibility (Table S2). All the scripts are available at https://gitlab.ifremer.fr/lgpmm/experimental_evolution.git.

Acknowledgment

We thank the staff of the Ifremer station at La Tremblade (ASIM), Frédéric Girardin and his team (Plateforme des Mollusques Marins de La Tremblade PMMLT), and Virginie François and his team (Plateforme des Mollusques Marins de Bouin PMMB). We also thank the SEBIMER team for maintaining bioinformatics tools.

C.P. was financially supported by a grant from the Ifremer Scientific Board and the Nouvelle-Aquitaine region. The present study was supported by scientific direction of Ifremer in context of the GT Huître project and by the FEAMP Gestinnov (FFEA470020FA1000007) GESTINNOV project and by DGAL (French General Directorate for Food) through the National Reference Laboratory for Mollusc Diseases and by the European-Union Reference Laboratory for Mollusc Diseases, Ifremer, La Tremblade. The authors acknowledge the Pôle de Calcul et de Données Marines (PCDM;

bioRxiv preprint doi: https://doi.org/10.1101/2025.02.07.637049; this version posted February 7, 2025. The copyright holder for this preprint (which was not certified by peer review) is the author/funder, who has granted bioRxiv a license to display the preprint in perpetuity. It is made available under aCC-BY-NC 4.0 International license.

https://wwz.ifremer.fr/en/Research-Technology/Research-Infrastructures/Digital-infrastructures/Computation-Centre) for providing DATARMOR computing and storage resources. The funders had no role in study design, data collection and interpretation, or the decision to submit the work for publication.

C.P. and co-authors thank J.M.E. for the discussions and exchanges. We would like to thank Bruno Petton and his team PHYTNESS for sampling the virus in the Brittany area, as well as Johan Vieira and the CAPENA team for sampling OsHV-1 in Arcachon Bay. B.M., N.F., and C.P. designed the study; L.D., B.M., and J.V.D. provided the biological materials; N.F., M.H., M.M., and C.P. collected and processed the samples. C.P. performed the bioinformatics analysis of the Illumina data. B.M., G.C., M.J., J.V.D., L.D., and C.P. drafted the manuscript. All authors read and approved the final version of the manuscript.

We declare that we have no competing interests.

bioRxiv preprint doi: https://doi.org/10.1101/2025.02.07.637049; this version posted February 7, 2025. The copyright holder for this preprint (which was not certified by peer review) is the author/funder, who has granted bioRxiv a license to display the preprint in perpetuity. It is made available under aCC-BY-NC 4.0 International license.

References

Abbadi, M., Zamperin, G., Gastaldelli, M., Pascoli, F., Rosani, U., Milani, A., Schivo, A., Rossetti, E., Turolla, E., Gennari, L., Toffan, A., Arcangeli, G., & Venier, P. (2018). Identification of a newly described OsHV-1 µvar from the North Adriatic Sea (Italy). *Journal of General Virology*, *99*(5), Article 5. https://doi.org/10.1099/jgv.0.001042

Anderson, R. M., & May, R. M. (1982). Coevolution of hosts and parasites. *Parasitology*, *85*(2), 411–426. https://doi.org/10.1017/S0031182000055360

Azéma, P., Lamy, J.-B., Boudry, P., Renault, T., Travers, M.-A., & Dégremont, L. (2017). Genetic parameters of resistance to Vibrio aestuarianus, and OsHV-1 infections in the Pacific oyster, Crassostrea gigas, at three different life stages. *Genetics, Selection, Evolution : GSE*, *49*, 23. https://doi.org/10.1186/s12711-017-0297-2

Azéma, P., Maurouard, E., Lamy, J.-B., & Dégremont, L. (2017). The use of size and growing height to improve Crassostrea gigas farming and breeding techniques against OsHV-1. *Aquaculture*, *471*, 121–129. https://doi.org/10.1016/j.aquaculture.2017.01.011

Barghi, N., Hermisson, J., & Schlötterer, C. (2020). Polygenic adaptation: A unifying framework to understand positive selection. *Nature Reviews Genetics*, *21*(12), 769–781. https://doi.org/10.1038/s41576-020-0250-z

Boudry, P., Collet, B., Cornette, F., Hervouet, V., & Bonhomme, F. (2002). *High variance in reproductive success of the Pacific oyster žCrassostrea gigas, Thunberg/ revealed by microsatellite-based parentage analysis of multifactorial crosses*.

Brito, A. F., & Pinney, J. W. (2020). The evolution of protein domain repertoires: Shedding light on the origins of the Herpesviridae family. *Virus Evolution*, *6*(1), veaa001. https://doi.org/10.1093/ve/veaa001

Bromham, L. (2020). *Substitution Rate Analysis and Molecular Evolution*.

Burioli, E. A. V., Prearo, M., & Houssin, M. (2017). Complete genome sequence of Ostreid herpesvirus type 1 µVar isolated during mortality events in the Pacific oyster Crassostrea gigas in France and Ireland. *Virology*, *509*, 239–251. https://doi.org/10.1016/j.virol.2017.06.027

bioRxiv preprint doi: https://doi.org/10.1101/2025.02.07.637049; this version posted February 7, 2025. The copyright holder for this preprint (which was not certified by peer review) is the author/funder, who has granted bioRxiv a license to display the preprint in perpetuity. It is made available under aCC-BY-NC 4.0 International license.

626 Cain, G., Liu, O., Whittington, R. J., & Hick, P. M. (2021). Reduction in Virulence over Time in Ostreid
627 herpesvirus 1 (OsHV-1) Microvariants between 2011 and 2015 in Australia. *Viruses*, *13*(5), 946.
628 https://doi.org/10.3390/v13050946
629 Cuevas, J. M., Willemsen, A., Hillung, J., Zwart, M. P., & Elena, S. F. (2015). Temporal Dynamics of
630 Intrahost Molecular Evolution for a Plant RNA Virus. *Molecular Biology and Evolution*, *32*(5),
631 1132–1147. https://doi.org/10.1093/molbev/msv028
632 Danecek, P., Bonfield, J. K., Liddle, J., Marshall, J., Ohan, V., Pollard, M. O., Whitwham, A., Keane,
633 T., McCarthy, S. A., Davies, R. M., & Li, H. (2021). Twelve years of SAMtools and BCFtools.
634 *GigaScience*, *10*(2), giab008. https://doi.org/10.1093/gigascience/giab008
635 Davison, A. J., Trus, B. L., Cheng, N., Steven, A. C., Watson, M. S., Cunningham, C., Deuff, R.-M. L.,
636 & Renault, T. (2005). A novel class of herpesvirus with bivalve hosts. *Journal of General*
637 *Virology*, *86*(1), Article 1. https://doi.org/10.1099/vir.0.80382-0
638 de Lorgeril, J., Lucasson, A., Petton, B., Toulza, E., Montagnani, C., Clerissi, C., Vidal-Dupiol, J.,
639 Chaparro, C., Galinier, R., Escoubas, J.-M., Haffner, P., Dégremont, L., Charrière, G. M.,
640 Lafont, M., Delort, A., Vergnes, A., Chiarello, M., Faury, N., Rubio, T., … Mitta, G. (2018).
641 Immune-suppression by OsHV-1 viral infection causes fatal bacteraemia in Pacific oysters.
642 *Nature Communications*, *9*(1), Article 1. https://doi.org/10.1038/s41467-018-06659-3
643 Dégremont, L. (2011). Evidence of herpesvirus (OsHV-1) resistance in juvenile Crassostrea gigas
644 selected for high resistance to the summer mortality phenomenon. *Aquaculture*, *317*(1–4), 94–
645 98. https://doi.org/10.1016/j.aquaculture.2011.04.029
646 Dégremont, L., Bédier, E., Soletchnik, P., Ropert, M., Huvet, A., Moal, J., Samain, J.-F., & Boudry, P.
647 (2005). Relative importance of family, site, and field placement timing on survival, growth, and
648 yield of hatchery-produced Pacific oyster spat (Crassostrea gigas). *Aquaculture*, *249*(1), 213–
649 229. https://doi.org/10.1016/j.aquaculture.2005.03.046
650 Dégremont, L., Ernande, B., Bédier, E., & Boudry, P. (2007). Summer mortality of hatchery-produced
651 Pacific oyster spat (Crassostrea gigas). I. Estimation of genetic parameters for survival and
652 growth. *Aquaculture*, *262*(1), 41–53. https://doi.org/10.1016/j.aquaculture.2006.10.025

bioRxiv preprint doi: https://doi.org/10.1101/2025.02.07.637049; this version posted February 7, 2025. The copyright holder for this preprint (which was not certified by peer review) is the author/funder, who has granted bioRxiv a license to display the preprint in perpetuity. It is made available under aCC-BY-NC 4.0 International license.

653 Dégremont, L., Maurouard, E., Ledu, C., & Benabdelmouna, A. (2019). Synthesis of the "PLAN DE
654 SAUVEGARDE" using selected all-triploid oysters to reduce the shortage of spat in France due
655 to OsHV-1–associated mortality in Crassostrea gigas. *Aquaculture*, *505*, 462–472.
656 https://doi.org/10.1016/j.aquaculture.2019.03.014
657 Delmotte, J., Chaparro, C., Galinier, R., de Lorgeril, J., Petton, B., Stenger, P.-L., Vidal-Dupiol, J.,
658 Destoumieux-Garzon, D., Gueguen, Y., Montagnani, C., Escoubas, J.-M., & Mitta, G. (2020).
659 Contribution of Viral Genomic Diversity to Oyster Susceptibility in the Pacific Oyster Mortality
660 Syndrome. *Frontiers in Microbiology*, *11*. https://doi.org/10.3389/fmicb.2020.01579
661 Delmotte, J., Pelletier, C., Morga, B., Galinier, R., Petton, B., Lamy, J.-B., Kaltz, O., Avarre, J.-C.,
662 Jacquot, M., Montagnani, C., & Escoubas, J.-M. (2022). Genetic diversity and connectivity of
663 the Ostreid herpesvirus 1 populations in France: A first attempt to phylogeographic inference
664 for a marine mollusc disease. *Virus Evolution*, *8*(1), veac039.
665 https://doi.org/10.1093/ve/veac039
666 Dotto-Maurel, A., Pelletier, C., Morga, B., Jacquot, M., Faury, N., Dégremont, L., Bereszczynki, M.,
667 Delmotte, J., Escoubas, J.-M., & Chevignon, G. (2022). Evaluation of tangential flow filtration
668 coupled to long-read sequencing for ostreid herpesvirus type 1 genome assembly. *Microbial*
669 *Genomics*, *8*(11). https://doi.org/10.1099/mgen.0.000895
670 Duffy, S., Shackelton, L. A., & Holmes, E. C. (2008). Rates of evolutionary change in viruses: Patterns
671 and determinants. *Nature Reviews Genetics*, *9*(4), 267–276. https://doi.org/10.1038/nrg2323
672 Elena, S. F., & Lenski, R. E. (1997). LONG-TERM EXPERIMENTAL EVOLUTION IN
673 ESCHERICHIA COLI. VII. MECHANISMS MAINTAINING GENETIC VARIABILITY
674 WITHIN POPULATIONS. *Evolution; International Journal of Organic Evolution*, *51*(4),
675 1058–1067. https://doi.org/10.1111/j.1558-5646.1997.tb03953.x
676 Elena, S. F., & Sanjuán, R. (2005). Adaptive Value of High Mutation Rates of RNA Viruses: Separating
677 Causes from Consequences. *Journal of Virology*, *79*(18), 11555–11558.
678 https://doi.org/10.1128/JVI.79.18.11555-11558.2005
679 Evans, O., Hick, P., & Whittington, R. J. (2017). Detection of Ostreid herpesvirus -1 microvariants in
680 healthy Crassostrea gigas following disease events and their possible role as reservoirs of

bioRxiv preprint doi: https://doi.org/10.1101/2025.02.07.637049; this version posted February 7, 2025. The copyright holder for this preprint (which was not certified by peer review) is the author/funder, who has granted bioRxiv a license to display the preprint in perpetuity. It is made available under aCC-BY-NC 4.0 International license.

681 infection. *Journal of Invertebrate Pathology*, *148*, 20–33.
682 https://doi.org/10.1016/j.jip.2017.05.004
683 Farahpour, F., Saeedghalati, M., & Hoffmann, D. (2022). *MullerPlot: Generates Muller Plot from*
684 *Population/Abundance/Frequency Dynamics Data. R package version 0.1.3.* (Version 0.1.3)
685 [Computer software].
686 Froissart, R., Wilke, C. O., Montville, R., Remold, S. K., Chao, L., & Turner, P. E. (2004). Co-infection
687 Weakens Selection Against Epistatic Mutations in RNA Viruses. *Genetics*, *168*(1), 9–19.
688 https://doi.org/10.1534/genetics.104.030205
689 Fuandila, N. N., Gosselin-Grenet, A.-S., Tilak, M.-K., Bergmann, S. M., Escoubas, J.-M., Klafack, S.,
690 Lusiastuti, A. M., Yuhana, M., Fiston-Lavier, A.-S., Avarre, J.-C., & Cherif, E. (2022).
691 Structural variation turnovers and defective genomes: Key drivers for the in vitro evolution of
692 the large double-stranded DNA koi herpesvirus (KHV). *Peer Community Journal*, *2*, e44.
693 https://doi.org/10.24072/pcjournal.154
694 Gandon, S., & Michalakis, Y. (2000). Evolution of parasite virulence against qualitative or quantitative
695 host resistance. *Proceedings. Biological Sciences*, *267*(1447), 985–990.
696 https://doi.org/10.1098/rspb.2000.1100
697 Gawra, J., Valdivieso, A., Roux, F., Laporte, M., de Lorgeril, J., Gueguen, Y., Saccas, M., Escoubas, J.-
698 M., Montagnani, C., Destoumieux-Garzón, D., Lagarde, F., Leroy, M. A., Haffner, P., Petton,
699 B., Cosseau, C., Morga, B., Dégremont, L., Mitta, G., Grunau, C., & Vidal-Dupiol, J. (2023).
700 Epigenetic variations are more substantial than genetic variations in rapid adaptation of oyster
701 to Pacific oyster mortality syndrome. *Science Advances*, *9*(36), eadh8990.
702 https://doi.org/10.1126/sciadv.adh8990
703 Gu, J., Zhou, Z., & Wang, Y. (2021). Editorial: Evolutionary Mechanisms of Infectious Diseases.
704 *Frontiers in Microbiology*, *12*. https://doi.org/10.3389/fmicb.2021.667561
705 Kassambara, A., & Mundt, F. (2020). *Extract and Visualize the Results of Multivariate Data Analyses*
706 *[R package factoextra v1.0.7]*. https://rpkgs.datanovia.com/factoextra/index.html

bioRxiv preprint doi: https://doi.org/10.1101/2025.02.07.637049; this version posted February 7, 2025. The copyright holder for this preprint (which was not certified by peer review) is the author/funder, who has granted bioRxiv a license to display the preprint in perpetuity. It is made available under aCC-BY-NC 4.0 International license.

Katoh, K., Misawa, K., Kuma, K., & Miyata, T. (2002). MAFFT: A novel method for rapid multiple sequence alignment based on fast Fourier transform. *Nucleic Acids Research*, *30*(14), Article 14. https://doi.org/10.1093/nar/gkf436

Kawecki, T. J., Lenski, R. E., Ebert, D., Hollis, B., Olivieri, I., & Whitlock, M. C. (2012). Experimental evolution. *Trends in Ecology & Evolution*, *27*(10), 547–560. https://doi.org/10.1016/j.tree.2012.06.001

Kubinak, J. L., & Potts, W. K. (2013). Host resistance influences patterns of experimental viral adaptation and virulence evolution. *Virulence*, *4*(5), 410–418. https://doi.org/10.4161/viru.24724

Kun, Á., Hubai, A. G., Král, A., Mokos, J., Mikulecz, B. Á., & Radványi, Á. (2023). Do pathogens always evolve to be less virulent? The virulence–transmission trade-off in light of the COVID-19 pandemic. *Biologia Futura*, 1–12. https://doi.org/10.1007/s42977-023-00159-2

Kuny, C. V., Bowen, C. D., Renner, D. W., Johnston, C. M., & Szpara, M. L. (2020). In vitro evolution of herpes simplex virus 1 (HSV-1) reveals selection for syncytia and other minor variants in cell culture. *Virus Evolution*, *6*(1), veaa013. https://doi.org/10.1093/ve/veaa013

Kutnjak, D., Elena, S. F., & Ravnikar, M. (2017). Time-Sampled Population Sequencing Reveals the Interplay of Selection and Genetic Drift in Experimental Evolution of *Potato Virus Y*. *Journal of Virology*, *91*(16), e00690-17. https://doi.org/10.1128/JVI.00690-17

Lauring, A. S. (2020). Within-host Viral Diversity, a Window into Viral Evolution. *Annual Review of Virology*, *7*(1), 63–81. https://doi.org/10.1146/annurev-virology-010320-061642

Li, H., & Roossinck, M. J. (2004). Genetic Bottlenecks Reduce Population Variation in an Experimental RNA Virus Population. *Journal of Virology*, *78*(19), 10582–10587. https://doi.org/10.1128/JVI.78.19.10582-10587.2004

McCrone, J. T., & Lauring, A. S. (2018). Genetic bottlenecks in intraspecies virus transmission. *Current Opinion in Virology*, *28*, 20–25. https://doi.org/10.1016/j.coviro.2017.10.008

Montville, R., Froissart, R., Remold, S. K., Tenaillon, O., & Turner, P. E. (2005). Evolution of Mutational Robustness in an RNA Virus. *PLOS Biology*, *3*(11), e381. https://doi.org/10.1371/journal.pbio.0030381

bioRxiv preprint doi: https://doi.org/10.1101/2025.02.07.637049; this version posted February 7, 2025. The copyright holder for this preprint (which was not certified by peer review) is the author/funder, who has granted bioRxiv a license to display the preprint in perpetuity. It is made available under aCC-BY-NC 4.0 International license.

735 Morga, B., Jacquot, M., Pelletier, C., Chevignon, G., Dégremont, L., Biétry, A., Pepin, J.-F., Heurtebise,
736 S., Escoubas, J.-M., Bean, T. P., Rosani, U., Bai, C.-M., Renault, T., & Lamy, J.-B. (2021).
737 Genomic Diversity of the Ostreid Herpesvirus Type 1 Across Time and Location and Among
738 Host Species. *Frontiers in Microbiology*, *12*, 711377.
739 https://doi.org/10.3389/fmicb.2021.711377
740 Nicolas, J.-L., Comps, M., & Cochennec, N. (1992). *Herpes-like virus infecting Pacific oyster larvae.*
741 (1). *12*(1), Article 1.
742 NIH. (2007). Understanding Emerging and Re-emerging Infectious Diseases. In *NIH Curriculum*
743 *Supplement Series [Internet]*. National Institutes of Health (US).
744 https://www.ncbi.nlm.nih.gov/books/NBK20370/
745 Patterson, N., Price, A. L., & Reich, D. (2006). Population Structure and Eigenanalysis. *PLOS Genetics*,
746 *2*(12), e190. https://doi.org/10.1371/journal.pgen.0020190
747 Peck, K. M., & Lauring, A. S. (2018). Complexities of Viral Mutation Rates. *Journal of Virology*,
748 *92*(14), 10.1128/jvi.01031-17. https://doi.org/10.1128/jvi.01031-17
749 Pelletier, C., Chevignon, G., Faury, N., Arzul, I., Garcia, C., Chollet, B., Renault, T., Morga, B., &
750 Jacquot, M. (2023). *Genetic differentiation and host specialization among OsHV-1 infecting*
751 *two oyster species in France* [Preprint]. Evolutionary Biology.
752 https://doi.org/10.1101/2023.08.23.554398
753 Pepin, J. F., Riou, A., & Renault, T. (2008). Rapid and sensitive detection of ostreid herpesvirus 1 in
754 oyster samples by real-time PCR. *Journal of Virological Methods*, *149*(2), Article 2.
755 https://doi.org/10.1016/j.jviromet.2008.01.022
756 Pernet, F., Fuhrmann, M., Petton, B., Mazurié, J., Bouget, J.-F., Fleury, E., Daigle, G., & Gernez, P.
757 (2018). Determination of risk factors for herpesvirus outbreak in oysters using a broad-scale
758 spatial epidemiology framework. *Scientific Reports*, *8*(1), Article 1.
759 https://doi.org/10.1038/s41598-018-29238-4
760 Petton, B., Boudry, P., Alunno-Bruscia, M., & Pernet, F. (2015). Factors influencing disease-induced
761 mortality of Pacific oysters Crassostrea gigas. *Aquaculture Environment Interactions*, *6*(3),
762 Article 3. https://doi.org/10.3354/aei00125

bioRxiv preprint doi: https://doi.org/10.1101/2025.02.07.637049; this version posted February 7, 2025. The copyright holder for this preprint (which was not certified by peer review) is the author/funder, who has granted bioRxiv a license to display the preprint in perpetuity. It is made available under aCC-BY-NC 4.0 International license.

R Development Core Team. (2005). *R: A language and environment for statistical computing*. [Computer software]. http://www.R-project.org

Renault, T., Cochennec, R., Le Deuff, R. M., & Chollet, B. (1994). *HERPES-LIKE VIRUS INFECTING JAPANESE OYSTER (CRASSOSTREA GIGAS) SPAT*. 3.

Sanjuán, R. (2012). From Molecular Genetics to Phylodynamics: Evolutionary Relevance of Mutation Rates Across Viruses. *PLOS Pathogens*, *8*(5), e1002685. https://doi.org/10.1371/journal.ppat.1002685

Sanjuán, R., & Domingo-Calap, P. (2016). Mechanisms of viral mutation. *Cellular and Molecular Life Sciences*, *73*(23), 4433–4448. https://doi.org/10.1007/s00018-016-2299-6

Sanjuán, R., Nebot, M. R., Chirico, N., Mansky, L. M., & Belshaw, R. (2010). Viral Mutation Rates. *Journal of Virology*, *84*(19), 9733–9748. https://doi.org/10.1128/JVI.00694-10

Sanjuán, R., Pereira-Gómez, M., & Risso, J. (2016). Chapter 3—Genome Instability in DNA Viruses. In I. Kovalchuk & O. Kovalchuk (Eds.), *Genome Stability* (pp. 37–47). Academic Press. https://doi.org/10.1016/B978-0-12-803309-8.00003-3

Schikorski, D., Renault, T., Saulnier, D., Faury, N., Moreau, P., & Pépin, J.-F. (2011). Experimental infection of Pacific oyster Crassostrea gigas spat by ostreid herpesvirus 1: Demonstration of oyster spat susceptibility. *Veterinary Research*, *42*(1), Article 1. https://doi.org/10.1186/1297-9716-42-27

Spitzer, K., Pelizzola, M., & Futschik, A. (2020). Modifying the Chi-square and the CMH test for population genetic inference: Adapting to overdispersion. *The Annals of Applied Statistics*, *14*(1). https://doi.org/10.1214/19-AOAS1301

Stoltzfus, A., & Norris, R. W. (2016). On the Causes of Evolutionary Transition:Transversion Bias. *Molecular Biology and Evolution*, *33*(3), 595–602. https://doi.org/10.1093/molbev/msv274

Suquet, M., Kermoysan, G. de, Araya, R. G., Queau, I., Lebrun, L., Souchu, P. L., & Mingant, C. (2009). Anesthesia in Pacific oyster, Crassostrea gigas. *Aquatic Living Resources*, *22*(1), Article 1. https://doi.org/10.1051/alr/2009006

Valdivieso, A., Morga, B., Degremont, L., Mege, M., Courtay, G., Dorant, Y., Escoubas, J.-M., Gawra, J., de Lorgeril, J., Mitta, G., Cosseau, C., & Vidal-Dupiol, J. (2025). DNA methylation

bioRxiv preprint doi: https://doi.org/10.1101/2025.02.07.637049; this version posted February 7, 2025. The copyright holder for this preprint (which was not certified by peer review) is the author/funder, who has granted bioRxiv a license to display the preprint in perpetuity. It is made available under aCC-BY-NC 4.0 International license.

landscapes before and after Pacific Oyster Mortality Syndrome are different within and between resistant and susceptible *Magallana gigas*. *Science of The Total Environment*, *962*, 178385. https://doi.org/10.1016/j.scitotenv.2025.178385

van Sluijs, L., Pijlman, G. P., & Kammenga, J. E. (2017). Why do Individuals Differ in Viral Susceptibility? A Story Told by Model Organisms. *Viruses*, *9*(10), 284. https://doi.org/10.3390/v9100284

Wickham, H. (2009). *ggplot2: Elegant Graphics for Data Analysis*. Springer New York. https://doi.org/10.1007/978-0-387-98141-3

Xia, J., Bai, C., Wang, C., Song, X., & Huang, J. (2015). Complete genome sequence of Ostreid herpesvirus-1 associated with mortalities of Scapharca broughtonii broodstocks. *Virology Journal*, *12*(1), Article 1. https://doi.org/10.1186/s12985-015-0334-0

Zwart, M. P., & Elena, S. F. (2015). Matters of Size: Genetic Bottlenecks in Virus Infection and Their Potential Impact on Evolution. *Annual Review of Virology*, *2*(Volume 2, 2015), 161–179. https://doi.org/10.1146/annurev-virology-100114-055135